

Global Practical Node and Edge Synchronization in Kuramoto Networks: A Submodular Optimization Framework

Andrew Clark, *Member, IEEE*, Basel Alomair, *Member, IEEE*, Linda Bushnell, *Senior Member, IEEE* and Radha Poovendran, *Senior Member, IEEE*

Abstract—Synchronization underlies biological and man-made phenomena including memory and perception in the brain, coordinated motion of animal flocks, and stability of the power grid, and is often modeled through networks of phase-coupled oscillating nodes. Heterogeneity in the node dynamics, however, may prevent such networks from achieving the required level of synchronization. In order to guarantee synchronization, external inputs can be used to pin a subset of nodes to a reference frequency, while the remaining nodes are steered toward synchronization via local coupling. In this paper, we present a submodular optimization framework for selecting a set of nodes to act as external inputs in order to achieve synchronization from almost any initial network state. We derive threshold-based sufficient conditions for synchronization, and then prove that these conditions are equivalent to connectivity of a class of augmented network graphs. Based on this connection, we map the sufficient conditions for synchronization to constraints on submodular functions, leading to efficient algorithms with provable optimality bounds for selecting input nodes. We illustrate our approach via numerical studies of synchronization in networks from power systems, wireless networks, and neuronal networks.

I. INTRODUCTION

Synchronization plays a vital role in complex networks. Stable operation of the power grid requires synchronization of buses and generators to a common frequency [1]. Synchronized oscillations of neuronal firing provide a biological mechanism for aggregating information in perception [2] and memory [3]. Coordinated motion of animals [4] occurs when a common heading is achieved. The prevalence of synchronization across different application domains motivates the study of the basic principles underlying synchronization [5].

Phase-coupled oscillators have been proposed as a widely-applicable framework for studying synchronization [6]. In phase-coupled oscillator networks, the dynamics of each node's phase are determined by a diffusive coupling with its neighbors (typically assumed to be sinusoidal [7]), together with an intrinsic frequency. The sinusoidal coupling causes the node phases to approach synchronization, while the intrinsic frequency drives each node away from synchronization.

The existence and stability of synchronized states has been studied extensively in the literature [8], [9], [10], including

A. Clark, L. Bushnell, and R. Poovendran are with the Department of Electrical Engineering, University of Washington, Seattle, WA, 98195-2500. {awclark, lb2, rp3}@uw.edu

B. Alomair is with the Center for Cybersecurity, King Abdulaziz City for Science and Technology, Riyadh, Saudi Arabia. alomair@kacst.edu.sa

conditions based on the intrinsic frequencies, network topology, and degree of coupling between the nodes. An important case is synchronization in the presence of external inputs [11]. External inputs arise in applications including neuroscience, where they represent environmental stimuli [2] or deep brain stimulation [12]. From an engineering standpoint, by introducing external inputs that pin a subset of nodes to a desired phase and frequency, a network that does not synchronize in the absence of inputs can be driven to a synchronized state, thus facilitating stability and performance of the network.

Existing analytical approaches to introducing external inputs assume that the external input node is connected to all other nodes [13], or that the network has a specific topology such as a complete graph [14]. Developing sufficient conditions for synchronization using external inputs in networks with arbitrary topology is an open problem. Efficient algorithms for selecting a subset of input nodes in order to guarantee synchronization are also currently lacking.

In this paper, we present an optimization framework for selecting a subset of phase-coupled oscillators to act as external inputs in order to guarantee synchronization of the overall network. We formulate sufficient conditions for ensuring convergence of phase-coupled oscillators to a synchronized state from almost any initial state (i.e., except for a measure zero set of initial states). We then develop a submodular optimization framework for selecting a minimum-size set of input nodes to achieve a desired level of synchronization, with provable bounds on the optimality of the chosen input nodes. Our contributions are summarized as follows:

- We investigate two synchronization problems. The first problem is to ensure that the phases of all of the oscillators converge to fixed points that are within a desired bound of a given reference phase (practical node synchronization). The second problem is to guarantee that the phase differences of neighboring nodes converge to within a desired bound of each other (practical edge synchronization). In both problems, the node frequencies must converge to the same value.
- We derive a set of sufficient conditions for a given set of input nodes to achieve practical node or edge synchronization from almost any initial state. We interpret our conditions as each node achieving a desired level of synchronization if a threshold number of neighbors reaches that level of synchronization.
- We develop a submodular optimization framework for se-

lecting a set of input nodes to achieve these synchronization conditions. Our approach is to derive a connection between the threshold conditions and the connectivity of an augmented graph. Based on this connection, we map our sufficient conditions to constraints on submodular functions. We propose efficient algorithms for selecting input nodes to guarantee synchronization and analyze the optimality bounds of our algorithms.

- We evaluate our approach through a numerical study of synchronization in three classes of networks. First, we consider synchronization of power grids using the IEEE 14 Bus test case [15]. Second, we study synchronization in geometric random graphs, motivated by vehicle coordination and wireless network synchronization problems. Finally, we investigate synchronization of neuronal networks based on the *C. Elegans* dataset [16].

The rest of the paper is organized as follows. In Section II, we give an overview of the related work. Section III contains our system model and definitions of synchronization. Sufficient conditions for synchronization are presented in Section IV. In Section V, we describe our submodular optimization approach to selecting input nodes. Section VI contains our numerical study. In Section VII, we conclude the paper and discuss directions for future work.

II. RELATED WORK

The phase-coupled oscillator framework for modeling synchronization phenomena was introduced in the seminal work of Winfree [17]. The sinusoidally-coupled Kuramoto model was later introduced in [18]. Extensive studies have been performed on the mean-field behavior of the Kuramoto model with all-to-all coupling (i.e., each node is coupled to each other node) in the limit as the network size grows large [7].

Synchronization of the Kuramoto model with a finite number of oscillators and arbitrary connection topology was studied in [9]. The authors proved that convergence to the synchronized state is guaranteed when all nodes have identical intrinsic frequencies, and analyzed the feasibility and stability of synchronization under non-identical intrinsic frequencies. Stable equilibria of the Kuramoto model in finite networks, including both synchronized and non-synchronized states, were analyzed in [19]. More recently, the existence, uniqueness, and stability of partially synchronized states was studied in [20], with application to power networks [1]. These prior works considered synchronization in the absence of external inputs.

Synchronization in the presence of external inputs has achieved relatively less study. Numerical studies have estimated the region of attraction, defined as the set of initial states that converge to the desired state, of the Kuramoto model with inputs for the case of all-to-all coupling [21]. Sufficient conditions for synchronization when there is a single input node that is connected to all other nodes were presented in [13], [22], [14]. These works do not, however, consider synchronization with external inputs in networks with arbitrary topology, and do not propose methods for selecting a subset of input nodes.

In the preliminary version of this paper [23], a submodular optimization approach to selecting a minimum-size set of input

nodes to guarantee that all node phases are within a desired bound of a reference phase was presented. Selecting input nodes in order to ensure that the relative phase differences of neighboring nodes are within a desired bound, which is relevant to stability of power grids [1], was not considered.

Selecting external input nodes to achieve synchronization can be viewed as part of the broader area of selecting input nodes to control complex networks. Much recent work on selecting input nodes has focused on guaranteeing controllability of linear dynamics on the network [24], [25]. The assumption of linear dynamics, however, is not applicable to the nonlinear oscillators considered here.

Phase-coupled oscillators in general, and Kuramoto oscillators in particular, have found extensive applications. Coupled oscillators were initially used to model natural phenomena such as bird flocking [26] and fish schooling [4]. At the level of individual cells, phase-coupled oscillators also provide a framework for heart pacemakers [27] and neuronal networks [3]. The prevalence of phase-coupled oscillators in nature has inspired engineering techniques for formation control [4] and time synchronization [28]. The phases of buses and generators in the power grid have also been modeled using phase-coupled oscillators, in order to understand whether the grid maintains a required level of synchronization for stability [29].

III. MODEL AND PRELIMINARIES

In this section, we describe the system model and oscillator dynamics. We then define the notions of synchronization considered in this paper. Finally, we give a preliminary result that will be needed for the proof of Theorem 2 in Section IV.

A. System Model

A network of n oscillators, indexed in the set $V = \{1, \dots, n\}$ is considered. Each oscillator $v \in V$ has a neighbor set $N(v) \subseteq V$, consisting of the set of oscillators that are coupled to v . We assume that links are bidirectional, so that $u \in N(v)$ implies $v \in N(u)$. An edge (u, v) exists if $u \in N(v)$ and $v \in N(u)$. We let E denote the set of edges, and let $p = |E|$.

Each oscillator v has a time-varying phase $\theta_v(t)$. The vector of oscillator phases at time t is denoted $\theta(t) \in \mathbb{R}^n$. We assume that there are two types of oscillators, denoted *input* and *non-input* oscillators. We let A denote the set of input oscillators. The phases of the non-input oscillators follow the Kuramoto dynamics

$$\dot{\theta}_v(t) = - \sum_{u \in N(v)} K_{uv} \sin(\theta_v(t) - \theta_u(t)) + \omega_v. \quad (1)$$

In (1), the first term represents the coupling between the oscillators, while ω_v is the intrinsic frequency of oscillator v and describes the phase dynamics in the absence of coupling. The coupling coefficient $K_{uv} > 0$ determines the relative strength of the two terms. We assume throughout that the couplings between nodes are symmetric, so that $K_{uv} = K_{vu}$ for all $(u, v) \in E$. We define $\bar{K}_v \triangleq \sum_{u \in N(v)} K_{uv}$.

Each input oscillator $v \in A$ is assumed to be pinned to a desired frequency ω_0 and phase offset θ_0 , so that $\dot{\theta}_v(t) = \omega_0$

and $\theta_v(t) = \omega_0 t + \theta_0$ for all $v \in A$. The overall oscillator dynamics are given by

$$\dot{\theta}_v(t) = \begin{cases} -\sum_{u \in N(v)} K_{uv} \sin(\theta_v(t) - \theta_u(t)) + \omega_v, & v \notin A \\ \omega_0, & v \in A \end{cases} \quad (2)$$

We define a function $f(x) : [-2\pi, 2\pi] \rightarrow [-\pi, \pi]$ as

$$f(x) = \begin{cases} x + 2\pi, & x \in [-2\pi, -\pi) \\ x, & x \in [-\pi, \pi) \\ x - 2\pi, & x \in [\pi, 2\pi] \end{cases}$$

The function $f(x)$ maps elements in $[-2\pi, 2\pi]$ into $[-\pi, \pi]$ while satisfying $\sin(f(x)) = \sin(x)$ and $\cos(f(x)) = \cos(x)$ for all x . This function will be used to define the edge cohesiveness property in the following subsection.

B. Definitions of Synchronization

We now define the notions of synchronization considered in this paper. Analogous definitions for networks without external inputs are given in [20].

The strongest form of synchronization is *phase synchronization*, defined as follows.

Definition 1: The oscillators achieve *phase synchronization* if there exists θ^* such that $\lim_{t \rightarrow \infty} \theta_v(t) = \theta^*$ for all $v \in V$.

Phase synchronization is achieved if all oscillators converge to the same phase. Since synchronization of all oscillators to the same phase is not possible in general [9], weaker notions of synchronization have been proposed. We first define *node- and edge-cohesiveness* as follows.

Definition 2 (Node Cohesiveness): A network of oscillators achieves *node cohesiveness* with parameter $\gamma \in [0, \frac{\pi}{4}]$ if there exists $T > 0$ such that, for all $t \geq T$, $|\theta_v - (\omega_0 t + \theta_0)| < \gamma$.

Definition 3 (Edge Cohesiveness): A network of oscillators achieves *edge cohesiveness* with parameter $\gamma \in [0, \frac{\pi}{2}]$ if there exists $T > 0$ such that, for all $t \geq T$ and all $(u, v) \in E$, $|f(\theta_v - \theta_u)| < \gamma$.

Node cohesiveness is achieved if all nodes converge to within a desired bound of the reference phase. Edge cohesiveness implies that the relative differences between any pair of neighboring nodes is bounded above. In general, node cohesiveness is desirable in applications such as coordinated motion [4] and time synchronization [28], where all nodes must agree on a common phase. Edge cohesiveness is desirable in applications including power systems [1], where the relative differences between nodes must be within a certain range to ensure stability.

We observe that a network that is node cohesive with parameter γ is edge cohesive with parameter 2γ . Indeed, node cohesiveness implies that there exists $T > 0$ such that, for all $t \geq T$,

$$\begin{aligned} |\theta_v(t) - \theta_u(t)| &= |(\theta_v(t) - (\omega_0 t + \theta_0)) - (\theta_u(t) - (\omega_0 t + \theta_0))| \\ &\leq |\theta_v(t) - (\omega_0 t + \theta_0)| + |\theta_u(t) - (\omega_0 t + \theta_0)| \\ &< \gamma + \gamma = 2\gamma. \end{aligned}$$

An additional synchronization notion is frequency synchronization, defined as follows.

Definition 4 (Frequency Synchronization): The oscillators achieve *frequency synchronization* if there exists ω^* such that $\lim_{t \rightarrow \infty} \dot{\theta}_v(t) = \omega^*$ for all $v \in V$.

Note that the only possible value for ω^* in Definition 4 is the frequency of the input nodes, denoted ω_0 , since we have $\dot{\theta}_v(t) \equiv \omega_0$ for all $v \in A$ and $t > 0$.

We now define the main types of synchronization considered in this paper.

Definition 5 (Practical Node and Edge Synchronization): The oscillators achieve *practical node synchronization* with parameter γ if they achieve frequency synchronization and node cohesiveness with parameter γ . The oscillators achieve *practical edge synchronization* with parameter γ if they achieve frequency synchronization and edge cohesiveness with parameter γ .

The following lemma allows us to focus on the case where $\omega_0 = 0$, so that all input oscillators have frequency 0.

Lemma 1: Define $\hat{\theta}(t) = \theta(t) - (\omega_0 t + \theta_0)\mathbf{1}$, where $\mathbf{1}$ denotes the vector of all 1's. Then $\theta(t)$ achieves practical node (resp. edge) synchronization with frequency ω_0 , phase bound γ , and reference frequency θ_0 if and only if $\hat{\theta}(t)$ achieves practical node (resp. edge) synchronization with frequency 0 and phase bound γ .

Proof: First, note that $\dot{\hat{\theta}}_v(t) = \dot{\theta}_v(t) - \omega_0$ for all $v \in V$. Suppose that $\theta(t)$ achieves practical node synchronization with frequency ω_0 , reference phase θ_0 , and phase bound γ . Then for all $v \in V$,

$$\lim_{t \rightarrow \infty} \dot{\hat{\theta}}_v(t) = \lim_{t \rightarrow \infty} (\dot{\theta}_v(t) - \omega_0) = 0.$$

Furthermore, there exists $T > 0$ such that, for all $t \geq T$ and $v \in V$,

$$|\hat{\theta}_v(t)| = |\theta_v(t) - (\theta_0 + \omega_0 t)| \leq \gamma,$$

and hence practical node synchronization is achieved. The proof for practical edge synchronization is similar, as is the proof of the converse. \blacksquare

C. Preliminary Result

The following preliminary result of [30] will be needed in Section IV. First, for any $\delta > 0$ and any matrix B , the δ -digraph is defined as the digraph where edge (i, j) exists if $B_{ij} \geq \delta$.

Theorem 1 ([30], Theorem 1): Consider the linear system $\dot{x}(t) = A(t)x(t)$, where $A(t)$ is a time-varying system matrix. Assume that the system matrix is a bounded piecewise continuous function of time, and that for every time t the system matrix is Metzler (i.e., all off-diagonal elements are nonnegative) and has zero row sums. Suppose further that there is an index $k \in \{1, \dots, n\}$, a threshold value $\delta > 0$, and an interval length $T > 0$ such that for all $t \in \mathbb{R}$ the δ -digraph associated to

$$\int_t^{t+T} A(s) \, ds$$

has the property that all nodes may be reached from the node k . Then the set of states $\{x^* \mathbf{1} : x^* \in \mathbb{R}\}$ is uniformly exponentially stable. In particular, all components of any solution converge to a common value as $t \rightarrow \infty$.

The theorem gives a sufficient condition for a linear system with time-varying weights to converge to consensus. Theorem 1 will be used to prove that, under certain conditions on the oscillator phases, the frequencies $\{\dot{\theta}_v(t) : v \in V\}$ converge to the frequencies of the input nodes.

IV. SUFFICIENT CONDITIONS FOR PRACTICAL SYNCHRONIZATION

In this section, we provide sufficient conditions for a set of inputs to achieve practical synchronization. We first show that the oscillators achieve practical node (resp. edge) synchronization if there exists at least one stable equilibrium point satisfying node (resp. edge) cohesiveness, and no stable equilibria that do not satisfy node (resp. edge) cohesiveness. We then formulate sufficient conditions for existence of a stable and cohesive equilibrium point, as well sufficient conditions for non-existence of stable equilibria that do not satisfy cohesiveness. We provide efficient algorithms for verifying the sufficient conditions for a given set of inputs.

A. Equilibrium Analysis and Practical Synchronization

As a preliminary, we define *node cohesive*, *edge cohesive*, *node non-cohesive*, and *edge non-cohesive* equilibria as follows.

Definition 6 (Cohesive and Non-cohesive Equilibria):

An equilibrium $\boldsymbol{\theta}^*$ of the dynamics (2) is *node cohesive* if $|\theta_v^*| \leq \gamma$ for all $v \in V$ and *edge cohesive* if $|\theta_v^* - \theta_u^*| \leq \gamma$ for all $(u, v) \in E$. An equilibrium is *node non-cohesive* if it is not node-cohesive, and *edge non-cohesive* if it is not edge-cohesive.

We first prove that the dynamics (2) are guaranteed to converge to an equilibrium point if an equilibrium exists. An analogous result is known in the case where there are no input nodes [21].

Lemma 2: Let Θ denote the set of equilibria of (2). If $\Theta \neq \emptyset$, then for any initial state $\boldsymbol{\theta}(0)$, there exists $\boldsymbol{\theta}^* \in \Theta$ such that $\lim_{t \rightarrow \infty} \boldsymbol{\theta}(t) = \boldsymbol{\theta}^*$.

Proof: Define $E_1 \triangleq \{(u, v) \in E : u \notin A, v \notin A\}$ and $E_2 \triangleq \{(u, v) \in E : u \in A, v \notin A\}$. Let $U(\boldsymbol{\theta}) : \mathbb{R}^n \rightarrow \mathbb{R}$ be given by

$$U(\boldsymbol{\theta}) = \sum_{(u, v) \in E_1} K_{uv} (1 - \cos(\theta_v - \theta_u)) + \sum_{(u, v) \in E_2} K_{uv} (1 - \cos \theta_v) - \sum_{v \notin A} \omega_v \theta_v.$$

The function U is continuously differentiable as a function of $\boldsymbol{\theta}$. We have that $\dot{\boldsymbol{\theta}} = -\nabla_{\boldsymbol{\theta}} U(\boldsymbol{\theta})$, and therefore $\dot{U}(\boldsymbol{\theta}) = -\|\dot{\boldsymbol{\theta}}\|_2^2$. Hence $\dot{U}(\boldsymbol{\theta}) \leq 0$ and $\dot{U}(\boldsymbol{\theta}) = 0$ if and only if $\boldsymbol{\theta}$ is an equilibrium, and we have $\{\boldsymbol{\theta} : \dot{U}(\boldsymbol{\theta}) = 0\} = \Theta$.

Since Θ is the set of equilibria of (2), it is invariant under the dynamics of (2). The lemma follows from LaSalle's Theorem [31]. \blacksquare

Lemma 2 implies that all initial states will converge to an equilibrium if at least one equilibrium exists. Furthermore, if $\boldsymbol{\theta}^*$ is an unstable equilibrium, then its stable manifold will have dimension less than n by the stable manifold theorem

[31], and hence the set of initial states that converge to $\boldsymbol{\theta}^*$ will have measure zero. Based on this observation and Lemma 2, we have the following theorem.

Theorem 2: Suppose that the dynamics (2) has at least one stable node cohesive (resp. edge cohesive) equilibrium and no stable non-node cohesive (resp. non-edge cohesive) equilibria. Then the oscillators achieve practical node (resp. edge) synchronization from almost any initial state.

Proof: Let Θ' denote the set of asymptotically stable equilibria of (2). Lemma 2 and the above discussion imply that, for almost all initial states, $\boldsymbol{\theta}(t)$ converges to an equilibrium in Θ' .

Suppose first that at least one stable equilibrium exists, and that all stable equilibria are node-cohesive. We show that node cohesiveness holds. Let $\bar{\theta} = \max \{|\theta_v| : v \in V, \boldsymbol{\theta} \in \Theta'\}$. We have $\bar{\theta} < \gamma$. Since the set of limit points of $\boldsymbol{\theta}(t)$ is contained in Θ' , for any solution $\boldsymbol{\theta}(t)$ to (2), $\lim_{t \rightarrow \infty} \boldsymbol{\theta}(t) = \boldsymbol{\theta}^*$ for some $\boldsymbol{\theta}^* \in \Theta'$. Hence there exists T such that $t > T$ implies that $|\theta_v(t) - \theta_v^*| < \gamma - \bar{\theta}$ for all $v \in V$. We then have

$$|\theta_v(t)| \leq |\theta_v^*| + |\theta_v(t) - \theta_v^*| < \bar{\theta} + \gamma - \bar{\theta} = \gamma.$$

Now, suppose that all stable equilibria are edge-cohesive. Let $\bar{\theta} = \max \{|\theta_v^* - \theta_u^*| : (u, v) \in E, \boldsymbol{\theta}^* \in \Theta'\}$. Since Θ' is the set of limit points of (2), every trajectory of (2) satisfies $|\theta_v(t) - \theta_u(t) - (\theta_v^* - \theta_u^*)| < \gamma - \bar{\theta}$ for t sufficiently large. Hence

$$|\theta_v(t) - \theta_u(t)| \leq |\theta_v^* - \theta_u^*| + |\theta_v(t) - \theta_u(t) - (\theta_v^* - \theta_u^*)| < \bar{\theta} + \gamma - \bar{\theta} = \gamma.$$

We now establish that frequency synchronization holds in both cases. Consider $\dot{\boldsymbol{\theta}}(t)$, which has dynamics

$$\ddot{\theta}_v(t) = - \sum_{u \in N(v)} \left[K_{uv} \cos(\theta_v(t) - \theta_u(t)) (\dot{\theta}_v(t) - \dot{\theta}_u(t)) \right] \quad (3)$$

for $v \notin A$ and $\ddot{\theta}_v(t) \equiv 0$ for $v \in A$. We now define dynamics of the form in Theorem 1 in order to analyze the convergence of (3). Let $x(t) \in \mathbb{R}^{n+1}$ denote the state variable, where x_{n+1} is a “super node” with dynamics $\dot{x}_{n+1}(t) \equiv 0$. Define the system matrix $A(t)$ by

$$A_{ij}(t) = \begin{cases} \cos K_{ij}(\theta_i(t) - \theta_j(t)), & (i, j) \in E, \\ -\sum_{j \in N(i)} K_{ij} \cos(\theta_i(t) - \theta_j(t)), & i \notin A \\ -1, & i = j, i \notin A \\ 1, & i = j, i \in A \\ 0, & i \in A, j = (n+1) \\ 0, & i = n+1 \end{cases}$$

By the preceding analysis, for both node- and edge-cohesive equilibria, there exists $T > 0$ such that $|\theta_i(t) - \theta_j(t)| < \pi/2$ for all $t > T$. Hence $A(t)$ is a bounded, piecewise continuous Metzler matrix with rows that sum to zero, and the node $(n+1)$ is connected to all other nodes in the associated δ -digraph. By Theorem 1, $x(t)$ converges to a state $x^* \mathbf{1}$.

Now, if we set $x_v(0) = x_{n+1} = 0$ for all $v \in A$ and $x_v(0) = \theta_v(0)$ for all $v \notin A$, then the trajectory of $[x_1(t) \cdots x_n(t)]^T$ will be identical to the trajectory of $\boldsymbol{\theta}(t)$. Since this is a special case of the more general result in the preceding paragraph, we

have that $\lim_{t \rightarrow \infty} \dot{\theta}(t) = \omega^* \mathbf{1}$ for some $\omega^* \in \mathbb{R}$. Moreover, since $\dot{\theta}_v(t) \equiv 0$ for all $v \in A$, we must have $\omega^* = 0$, implying frequency synchronization. \blacksquare

Theorem 2 implies that, in order to prove that practical node (resp. edge) synchronization is achieved from almost any initial state, it suffices to show that there is at least one stable node-cohesive (resp. edge-cohesive) equilibrium and no stable non-cohesive equilibria. Sufficient conditions for these two properties are derived in the following two subsections.

B. Existence of Cohesive Stable Equilibria

In this section, we first demonstrate that any node or edge cohesive equilibrium is stable. We then present a sufficient condition for the existence of a cohesive equilibrium. As a preliminary, we consider the Jacobian of the non-input oscillator dynamics:

$$J_{uv} = \begin{cases} K_{uv} \cos(\theta_u - \theta_v), & (u, v) \in E, \\ -\sum_{u \in N(v) \setminus A} K_{uv} \cos(\theta_u - \theta_v) & u, v \notin A \\ -\sum_{u \in N(v) \cap A} K_{uv} \cos \theta_v, & u = v \\ 0, & \text{else} \end{cases} \quad (4)$$

Lemma 3: All node- and edge-cohesive equilibria are asymptotically stable.

Proof: Let $\boldsymbol{\theta}^*$ be a node cohesive equilibrium. Since $|\theta_v^*| < 2\gamma < \pi/2$ and $|\theta_u^* - \theta_v^*| < \gamma \leq \pi/2$, $\cos(\theta_v^* - \theta_u^*) \geq 0$ for all $(u, v) \in E$ and $\cos(\theta_v^*) \geq 0$ for all v . Similarly, if $\boldsymbol{\theta}^*$ is an edge cohesive equilibrium, then $|\theta_u - \theta_v| \leq \gamma$ and so $\cos(\theta_v^* - \theta_u^*) \geq 0$ for all $(u, v) \in E$. In both cases, J is negative definite, and hence the equilibrium is stable. \blacksquare

Since any cohesive equilibrium is stable by Lemma 3, it suffices to show that at least one cohesive equilibrium exists. The following theorem gives sufficient conditions for existence of node-cohesive and edge-cohesive equilibria for a given set of input nodes.

Theorem 3: Let $\{\bar{\theta}_v : v \in V\}$ and $\{\bar{\theta}_{uv} : (u, v) \in E\}$ be sets of nonnegative real numbers. Define

$$\begin{aligned} \Lambda = \{\boldsymbol{\theta} : |\theta_v| \leq \bar{\theta}_v \ \forall v \in V\} \\ \cap \{\boldsymbol{\theta} : |f(\theta_v - \theta_u)| \leq \bar{\theta}_{uv} \ \forall (u, v) \in E\}, \end{aligned}$$

where f is defined in Section III-A. Suppose that for all $\boldsymbol{\theta} \in \Lambda$ with $\boldsymbol{\theta} = (\theta_1, \dots, \bar{\theta}_v, \dots, \theta_n)$,

$$\sum_{u \in N(v)} K_{uv} \sin(\bar{\theta}_v - \theta_u) > |\omega_v|$$

and that for all $\boldsymbol{\theta} \in \Lambda$ with $(\theta_v - \theta_u) = \bar{\theta}_{uv}$,

$$K_{uv} \sin \bar{\theta}_{uv} + \sum_{\hat{u} \in N(v) \setminus \{u\}} K_{\hat{u}v} \sin(\theta_v - \theta_{\hat{u}}) > |\omega_v|.$$

Then there exists an equilibrium in Λ .

Proof: The approach of the proof is to show that Λ is a positive invariant set and apply Brouwer's fixed point theorem [32] to show existence of an equilibrium point. Suppose that Λ is not positive invariant. For some trajectory of (2) with

$\boldsymbol{\theta}(0) \in \Lambda$, let $t^* = \inf \{t : \boldsymbol{\theta}(t) \notin \Lambda\}$. Define $\bar{V} = \{v \in V : |\theta_v(t^*)| = \bar{\theta}_v\}$, and consider $v \in \bar{V}$. If $\theta_v(t^*) = \bar{\theta}_v$, then

$$\begin{aligned} \dot{\theta}_v(t^*) &= - \sum_{u \in N(v)} K_{uv} \sin(\theta_v(t^*) - \theta_u(t^*)) + \omega_v \\ &= - \sum_{u \in N(v)} K_{uv} \sin(\bar{\theta}_v - \theta_u(t^*)) + \omega_v \\ &< -|\omega_v| + \omega_v \leq 0 \end{aligned}$$

where the final inequality follows from the assumption of the theorem and the fact that $\boldsymbol{\theta}(t^*)$ is on the boundary of Λ by continuity of $\boldsymbol{\theta}(t)$. Since $\dot{\theta}_v(t^*) < 0$, there exists $\epsilon(v)$ such that $|\theta_v(t)| \leq \bar{\theta}_v$ for $t \in [t^*, t^* + \epsilon(v)]$. Similarly, if $\theta_v(t^*) = -\bar{\theta}_v$, we have

$$\begin{aligned} \dot{\theta}_v(t^*) &= - \sum_{u \in N(v)} K_{uv} \sin(-\bar{\theta}_v - \theta_u(t^*)) + \omega_v \\ &= \sum_{u \in N(v)} K_{uv} \sin(\bar{\theta}_v - (-\theta_u(t^*))) + \omega_v \\ &> |\omega_v| + \omega_v \geq 0 \end{aligned}$$

where the inequality follows from the fact that $\boldsymbol{\theta} \in \Lambda$ implies $-\boldsymbol{\theta} \in \Lambda$.

Now, suppose that $\theta_v(t^*) - \theta_u(t^*) = \bar{\theta}_{uv}$. Then we have

$$\begin{aligned} \frac{d}{dt}(\theta_v(t^*) - \theta_u(t^*)) &= \omega_v - K_{uv} \sin(\theta_v(t^*) - \theta_u(t^*)) \\ &\quad - \sum_{\hat{u} \in N(v) \setminus \{u\}} K_{\hat{u}v} \sin(\theta_v(t^*) - \theta_{\hat{u}}(t^*)) \\ &\quad + K_{uv} \sin(\theta_u(t^*) - \theta_v(t^*)) - \omega_u \\ &\quad + \sum_{\hat{v} \in N(u) \setminus \{v\}} K_{u\hat{v}} \sin(\theta_u(t^*) - \theta_{\hat{v}}(t^*)) \\ &= \omega_v - K_{uv} \sin \bar{\theta}_{uv} \\ &\quad - \sum_{\hat{u} \in N(v) \setminus \{u\}} K_{\hat{u}v} \sin(\theta_v(t) - \theta_{\hat{u}}(t)) + \omega_u - K_{uv} \sin \bar{\theta}_{uv} \\ &\quad + \sum_{\hat{v} \in N(u) \setminus \{v\}} K_{u\hat{v}} \sin(\theta_u(t^*) - \theta_{\hat{v}}(t^*)) \\ &< -|\omega_v| + \omega_v - |\omega_u| + \omega_u \leq 0 \end{aligned}$$

and hence $(\theta_v(t) - \theta_u(t))$ is decreasing in a neighborhood of t^* .

Putting the arguments of the preceding paragraphs together, we have that there exists $\epsilon > 0$ such that $t \in [t^*, t^* + \epsilon]$ implies that $\boldsymbol{\theta} \in \Lambda$, contradicting the definition of t^* . Hence if $\boldsymbol{\theta}(0) \in \Lambda$, then $\boldsymbol{\theta}(t) \in \Lambda$ for all $t \geq 0$, implying that Λ is positive invariant. Since Λ is compact, convex, and positive invariant, it contains an equilibrium [32]. \blacksquare

Theorem 3 is a threshold-based condition for existence of cohesive equilibria. If a sufficient number of neighbors of node v lie in the cohesive region, then node v will remain in the cohesive region. The following corollary gives explicit conditions for existence of node and edge cohesive equilibria.

Corollary 1: If there exist $\{\bar{\theta}_v : v \in V\}$ and $\{\bar{\theta}_{uv} : (u, v) \in E\}$ satisfying the conditions of Theorem 3 with $|\bar{\theta}_v| \leq \gamma$ for all $v \in V$, then there is a node cohesive equilibrium. If there exist $\{\bar{\theta}_v : v \in V\}$ and $\{\bar{\theta}_{uv} : (u, v) \in E\}$ satisfying the conditions of Theorem 3 with $\bar{\theta}_{uv} \leq \gamma$ for all $(u, v) \in E$, then there exists an edge cohesive equilibrium.

Theorem 3 and Corollary 1 give sufficient conditions for existence of a stable cohesive equilibrium point. In the following section, we provide an algorithm for verifying the existence of such equilibria based on these conditions.

C. Verifying Existence of Node- and Edge-Cohesive Equilibria

In this section, we provide an algorithm for verifying the existence of stable cohesive equilibria. The goal of the algorithm is to identify sets $\{\bar{\theta}_v : v \in V \setminus A\}$ and $\{\bar{\theta}_{uv} : (u, v) \in E\}$ satisfying the conditions of Theorem 3. The approach consists of a contraction-based method to identify a feasible region Λ for the set of fixed points, and then prove that the conditions of Theorem 3 are satisfied. As a preliminary, define weights $\beta_1(m, l)$, $\beta_2(m, l)$, and $\beta_3(m, l)$ by

$$\begin{aligned}\beta_1(m, l) &= \min \left\{ \sin(\theta_v - \theta_u) : \theta_v \in \left[\frac{\gamma(m-1)}{M}, \frac{\gamma m}{M} \right], \right. \\ &\quad \left. |\theta_u| \leq \frac{\gamma l}{M} \right\} \\ \beta_2(r) &= \min \left\{ \sin(\theta) : |\theta| \in \left[\frac{\gamma(r-1)}{M}, \frac{\gamma r}{M} \right] \right\} \\ \beta_3(r) &= \min \left\{ \sin(\theta) : |\theta| \leq \frac{\gamma r}{M} \right\}\end{aligned}$$

In the algorithm, we select $M \in \mathbb{Z}^+$ and initialize a set $S = A$. The algorithm maintains a set of time-varying weights $\{x_v[k] : v \in V\} \cup \{x_{uv}[k] : (u, v) \in E\}$. The initialization of the weights $\{x_v[0] : v \in V\}$ is given as $x_v[0] = 0$ if $v \in A$ and $x_v[0] = M$ if $v \notin A$. For the weights $\{x_{uv}[0] : (u, v) \in E\}$, the initialization is given as $x_{uv}[0] = 0$ if $u \in A$ and $v \in A$, $x_{uv}[0] = M$ otherwise.

At each iteration k of the algorithm, loop over all nodes $v \in V \setminus A$ and check whether

$$\sum_{u \in N(v)} K_{uv} \beta_1(x_v[k-1], x_u[k-1]) > |\omega_v|. \quad (5)$$

If (5) holds, set $x_v[k] = x_v[k-1] - 1$ and $S = S \cup \{v\}$. If (5) does not hold for any v , then loop over all edges $(u, v) \in E$ and check whether

$$\begin{aligned}\sum_{\hat{u} \in N(v) \setminus \{u\}} K_{\hat{u}v} \beta_3(x_{\hat{u}v}[k-1]) \\ + K_{uv} \beta_2(x_{uv}[k-1]) > |\omega_v| \quad (6)\end{aligned}$$

$$\begin{aligned}\sum_{\hat{v} \in N(u) \setminus \{v\}} K_{u\hat{v}} \beta_3(x_{u\hat{v}}[k-1]) \\ + K_{uv} \beta_2(x_{uv}[k-1]) > |\omega_u| \quad (7)\end{aligned}$$

If there exists $(u, v) \in E$ satisfying (6) and (7), set $x_{uv}[k] = x_{uv}[k-1] - 1$ and $S = S \cup \{(u, v)\}$. If no such edge exists, then the algorithm terminates.

The algorithm terminates after at most $M(n+p)$ iterations, since each x_v and x_{uv} can be decremented at most M times. The following theorem relates the termination conditions of the algorithm to the sufficient condition of Theorem 3.

Theorem 4: If $S = V \cup E$ when the algorithm terminates, then node and edge cohesive equilibria exist. If \mathbf{x}^* denotes the

vector of weights when termination occurs, then there exists an equilibrium in

$$\Phi = \left\{ \boldsymbol{\theta} : |\theta_v| \leq \frac{x_v^* \gamma}{M} \right\} \cap \left\{ \boldsymbol{\theta} : |\theta_v - \theta_u| \leq \frac{x_{uv}^* \gamma}{M} \right\}.$$

Proof: Suppose that $V \subseteq S$ and let $v \in V \setminus A$. Define $\bar{\theta}_v = \frac{x_v^* \gamma}{M}$, and let $k_v = \min \{k : x_v^* = x_v[k]\}$. Then for any $|\theta_u| \leq \frac{x_u[k_v-1] \gamma}{M}$, we have

$$\begin{aligned}\sum_{u \in N(v)} K_{uv} \sin(\bar{\theta}_v - \theta_u) \\ \geq \min \left\{ \sum_{u \in N(v)} K_{uv} \sin(\bar{\theta}_v - \theta_u) : |\theta_u| \leq \frac{x_u[k_v-1] \gamma}{M} \right\} \\ = \sum_{u \in N(v)} K_{uv} \min \left\{ \sin(\bar{\theta}_v - \theta_u) : |\theta_u| \leq \frac{x_u[k_v-1] \gamma}{M} \right\} \\ \geq \sum_{u \in N(v)} K_{uv} \beta_1(x_v[k_v-1], x_u[k_v-1]) > |\omega_v| \quad (8)\end{aligned}$$

where (8) follows from (5) and the definition of β_1 .

Now, suppose $E \subseteq S$ and let $(u, v) \in E$. Let $\bar{\theta}_{uv} = \frac{x_{uv}^* \gamma}{M}$, and let $k_{uv} = \min \{k : x_{uv}^* = x_{uv}[k]\}$. Then for all $(\hat{u}, \hat{v}) \in E$ satisfying $|\theta_{\hat{v}} - \theta_{\hat{u}}| \leq \frac{x_{\hat{u}\hat{v}}[k_{uv}-1] \gamma}{M}$, we have

$$\begin{aligned}\sum_{\hat{u} \in N(v)} K_{\hat{u}v} \sin(\theta_v - \theta_{\hat{u}}) \\ \geq \sum_{\hat{u} \in N(v) \setminus \{u\}} K_{\hat{u}v} \min \{ \sin(\theta_v - \theta_{\hat{u}}) : \\ |\theta_v - \theta_{\hat{u}}| \leq \frac{x_{\hat{u}v}[k_{uv}-1] \gamma}{M} \} + K_{uv} \sin(\bar{\theta}_{uv}) \\ \geq \sum_{\hat{u} \in N(v) \setminus \{u\}} K_{\hat{u}v} \beta_3(x_{\hat{u}v}[k_{uv}-1]) \\ + K_{uv} \beta_2(x_{uv}[k_{uv}-1]) \\ > |\omega_v| \quad (10)\end{aligned}$$

where (9) follows from the definition of β_2 and β_3 and (10) follows from (6). Since $x_{uv}[k_{uv}-1] \geq x_{uv}^*$ for all $(u, v) \in E$, the inequalities hold for all $\boldsymbol{\theta} \in \Phi$.

Combining the arguments of the preceding paragraphs implies that the conditions of Theorem 3 are satisfied for set Φ , and hence cohesive equilibria exist. ■

The algorithm presented in this section gives an approach for proving node and edge cohesiveness when an input set is given. In Section V-A, we formulate the problem of selecting a set of input nodes A that guarantees $S = V \cup E$, and hence guarantees existence of cohesive equilibrium.

D. Conditions for Non-Existence of Stable Non-Cohesive Equilibria

In this section, we first identify a sufficient condition for an equilibrium to be unstable. We then provide two sufficient conditions for non-existence of stable equilibria within a given region.

Lemma 4: Let $\boldsymbol{\theta}^*$ be an equilibrium point. Suppose that, for some $v \in V \setminus A$,

$$\sum_{u \in N(v)} \cos(\theta_v^* - \theta_u^*) < 0. \quad (11)$$

Then θ^* is unstable.

Proof: Consider the Jacobian matrix defined in (4). If (11) holds for some $v \in V \setminus A$, let e_v denote the vector with a 1 in index v and 0's elsewhere. Then $e_v^T J e_v > 0$, and hence the equilibrium θ^* is unstable. \blacksquare

In order to prove that all stable equilibria are cohesive, we must show that each subset of the non-cohesive region contains no stable equilibria. The following lemma formalizes this condition.

Lemma 5: Let $v \in V \setminus A$, and let $\bar{\theta}'_v$ and $\bar{\theta}_v$ be real numbers satisfying $0 < \bar{\theta}'_v < \bar{\theta}_v < \pi$. Furthermore, let $\{\bar{\theta}_u : u \in V \setminus \{v\}\}$ be a set of real numbers in $[0, \pi]$. Define

$$\Theta = \{\theta : \theta_v \in [\bar{\theta}'_v, \bar{\theta}_v], |\theta_u| \leq \bar{\theta}_u\}.$$

If there exists $\lambda \geq 0$ such that

$$\sum_{u \in N(v)} K_{uv} [\sin(\theta_v - \theta_u) - \lambda \cos(\theta_v - \theta_u)] > |\omega_v|$$

for all $\theta \in \Theta$, then there are no stable equilibria in Θ .

Proof: Observe that if, for all $\theta \in \Theta$,

$$\sum_{u \in N(v)} K_{uv} \sin(\theta_v - \theta_u) > |\omega_v|,$$

then there are no equilibria in Θ . Combining this with the condition of Lemma 4, we have that there are no stable equilibria if

$$\min \left\{ \sum_{u \in N(v)} K_{uv} \sin(\theta_v - \theta_u) : \sum_{u \in N(v)} K_{uv} \cos(\theta_v - \theta_u) > 0, \theta \in \Phi \right\} > |\omega_v|.$$

By lower-bounding the left-hand side using the Lagrange dual, we have that

$$\min_{\theta \in \Theta} \sum_{u \in N(v)} K_{uv} [\sin(\theta_v - \theta_u) - \lambda \cos(\theta_v - \theta_u)] > |\omega_v|$$

is sufficient for non-existence of a stable equilibrium point in the region Θ . \blacksquare

An analogous condition can be proved for a region Θ' defined by the relative phase differences between the nodes.

Lemma 6: Let $(u, v) \in E$, and let $\bar{\theta}'_{uv}$ and $\bar{\theta}_{uv}$ be real numbers satisfying $0 < \bar{\theta}'_{uv} < \bar{\theta}_{uv} < \pi$. Furthermore, let $\{\bar{\theta}_{\hat{u}\hat{v}} : (\hat{u}, \hat{v}) \in E\}$ be a set of real numbers in $[0, \pi]$. Define

$$\Theta' = \{\theta : |f(\theta_v - \theta_u)| \in [\bar{\theta}'_{uv}, \bar{\theta}_{uv}], |f(\theta_{\hat{v}} - \theta_{\hat{u}})| \leq \bar{\theta}_{\hat{u}\hat{v}}\}.$$

If there exists $\lambda \geq 0$ such that

$$\sum_{u \in N(v)} K_{uv} [\sin(\theta_v - \theta_u) - \lambda \cos(\theta_v - \theta_u)] > |\omega_v| \quad (12)$$

for all $\theta \in \Theta'$, then there are no stable equilibria in Θ' .

The proof is similar to Lemma 5 and is omitted. Lemmas 5 and 6 give conditions for non-existence of non-cohesive stable equilibria. In the next section, we present an algorithm for verifying that these conditions are satisfied.

E. Verifying Non-Existence of Stable Non-Cohesive Equilibria

In this section, we present an algorithm, analogous to the algorithm of Section IV-C, for verifying that there are no stable non-cohesive equilibria. As in Section IV-C, our approach is to consider the region where stable equilibria can occur, and reduce the size of the region at each iteration. We show that non-node cohesive equilibria as well as non-edge cohesive equilibria can be checked using this approach.

As a preliminary, we define weights β_1^λ , β_2^λ , and β_3^λ , for $\lambda \in [0, \infty]$, as follows.

$$\beta_1^\lambda(m, l) = \min \left\{ g_\lambda(\theta_v - \theta_u) : \theta_v \in \left[\frac{\pi(m-1)}{M}, \frac{\pi m}{M} \right], |\theta_u| \leq \frac{\pi l}{M} \right\},$$

$$\beta_2^\lambda(r) = \min \left\{ g_\lambda(\theta_v - \theta_u) : |f(\theta_v - \theta_u)| \leq \frac{\pi r}{M} \right\}$$

$$\beta_3^\lambda(r) = \min \left\{ g_\lambda(\theta_v - \theta_u) : |f(\theta_v - \theta_u)| \in \left[\frac{\pi(r-1)}{M}, \frac{\pi r}{M} \right] \right\}$$

with

$$g_\lambda(x) = \begin{cases} \sin(x) - \lambda \cos(x), & \lambda \in [0, \infty) \\ -\cos(x), & \lambda = \infty \end{cases}$$

The algorithm is defined as follows. Let $M \in \mathbb{Z}^+$ and define a set of time-varying indices $\{y_v[k] : v \in V\}$ and $\{y_{uv}[k] : (u, v) \in E\}$. The indices y_v are initialized as $y_v[0] = 0$ if $v \in A$ and $y_v[0] = M$ otherwise. The indices y_{uv} are initialized as $y_{uv}[0] = 0$ if $u \in A$, $v \in A$ and $y_{uv}[0] = M$ otherwise.

Choose a set $\Psi = \{\lambda_1, \dots, \lambda_R\} \subseteq [0, \infty]$. At each iteration of the algorithm, for each node $v \in V \setminus A$, check whether

$$\sum_{u \in N(v)} K_{uv} \beta_1^\lambda(y_v[k-1], y_u[k-1]) > \tau_{\lambda, v} \quad (13)$$

for some $\lambda \in \Psi$, where $\tau_{\lambda, v} = |\omega_v|$ for $\lambda \in [0, \infty)$ and $\tau_{\infty, v} = 0$. If v satisfies (13), set $y_v[k] = y_v[k-1] - 1$ and continue to the next iteration.

If no such node v exists, iterate over all edges $(u, v) \in E$ and check whether

$$K_{uv} \beta_3^\lambda(y_{uv}[k-1]) + \sum_{\hat{u} \in N(v) \setminus \{u\}} K_{\hat{u}v} \beta_2^\lambda(y_{\hat{u}v}[k-1]) > \tau_{\lambda, v} \quad (14)$$

$$K_{uv} \beta_3^\lambda(y_{uv}[k-1]) + \sum_{\hat{v} \in N(u) \setminus \{v\}} K_{u\hat{v}} \beta_2^\lambda(y_{u\hat{v}}[k-1]) > \tau_{\lambda, u} \quad (15)$$

where $\tau_{\lambda, v}$ and $\tau_{\lambda, u}$ are defined as in the previous paragraph. If (u, v) satisfies (14) and (15), set $y_{uv}[k] = y_{uv}[k-1] - 1$ and continue. If no such edge (u, v) exists, the algorithm terminates.

Since each index y_v and y_{uv} can be decremented at most M times, the algorithm terminates within $M(n+p)$ iterations. The

complexity of the algorithm depends on M , which determines the number of iterations, as well as $|\Psi|$, which determines the workload per iteration. Larger values of M and $|\Psi|$ will increase the complexity, but will also result in a tighter sufficient condition.

The following theorem establishes that the algorithm of this section verifies that no stable non-cohesive equilibria exist.

Theorem 5: Let \mathbf{y}^* denote the vector of indices upon termination. Define Φ^* as

$$\Phi^* \triangleq \left\{ \boldsymbol{\theta} : |\theta_v| \leq \frac{\pi y_v^*}{M} \forall v \in V, \right. \\ \left. |f(\theta_v - \theta_u)| \leq \frac{\pi y_{uv}^*}{M} \forall (u, v) \in E \right\}.$$

Then all stable equilibria lie in Φ .

Proof: Define

$$\Phi_k \triangleq \left\{ \boldsymbol{\theta} : |\theta_v| \leq \frac{\pi y_v[k]}{M} \forall v \in V, \right. \\ \left. |f(\theta_v - \theta_u)| \leq \frac{\pi y_{uv}[k]}{M} \forall (u, v) \in E \right\},$$

so that $\Phi_k \subseteq \Phi_{k-1}$. It suffices to show that at each iteration k , all stable equilibria lie in Φ_k . This result is trivially true when $k = 0$.

At $k > 0$, it suffices to show that there are no stable equilibria in $\Phi_{k-1} \setminus \Phi_k$. Suppose that v satisfies $y_v[k] = y_v[k-1] - 1$. Then

$$\Phi_{k-1} \setminus \Phi_k = \left\{ \boldsymbol{\theta} : |\theta_v| \in \left[\frac{\pi(y_v[k-1] - 1)}{M}, \frac{\pi y_v[k-1]}{M} \right], \right. \\ \left. |\theta_u| \leq \frac{\pi y_u[k-1]}{M}, |f(\theta_v - \theta_u)| \leq \frac{\pi y_{uv}[k-1]}{M} \right\}.$$

By (13), there exists $\lambda \in [0, \infty]$ such that, for all $\boldsymbol{\theta} \in \Phi_{k-1} \setminus \Phi_k$,

$$\sum_{u \in N(v)} K_{uv} [\sin(\theta_v - \theta_u) - \lambda \cos(\theta_v - \theta_u)] \quad (16)$$

$$\geq \min_{\boldsymbol{\theta} \in \Phi_{k-1} \setminus \Phi_k} \left\{ \sum_{u \in N(v)} K_{uv} [\sin(\theta_v - \theta_u) \right. \\ \left. - \lambda \cos(\theta_v - \theta_u)] \right\} \quad (17)$$

$$\geq \sum_{u \in N(v)} K_{uv} \beta_1^\lambda (y_v[k-1]) \quad (17)$$

$$> \tau_{\lambda, v} \quad (18)$$

where (17) follows from the definition of β_1^λ and (18) follows from (13). Hence the conditions of Lemma 5 are satisfied for $\Phi_{k-1} \setminus \Phi_k$, and so there are no stable equilibria in $\Phi_{k-1} \setminus \Phi_k$.

Now, suppose that $(u, v) \in E$ satisfies $y_{uv}[k] = y_{uv}[k-1] - 1$. We have that

$$\Phi_{k-1} \setminus \Phi_k = \left\{ \boldsymbol{\theta} : |\theta_v| \leq \frac{\pi y_v[k-1]}{M}, \right. \\ \left. |f(\theta_v - \theta_u)| \leq \frac{\pi y_{uv}[k-1]}{M}, \right. \\ \left. |f(\theta_v - \theta_u)| \in \left[\frac{\pi(y_{uv}[k-1] - 1)}{M}, \frac{\pi y_{uv}[k-1]}{M} \right] \right\}.$$

By (14) and (15), there exists λ such that

$$K_{uv} g_\lambda(\theta_v - \theta_u) + \sum_{\hat{u} \in N(v)} K_{\hat{u}v} g_\lambda(\theta_v - \theta_{\hat{u}}) > \tau_{\lambda, v},$$

and by Lemma 6 there are no stable equilibria in $\Phi_{k-1} \setminus \Phi_k$. Hence, by induction, all stable equilibria lie in Φ^* . \blacksquare

The following corollary gives explicit conditions for node and edge cohesiveness.

Corollary 2: If y_{uv}^* satisfies $\frac{y_{uv}^* \pi}{M} \leq \gamma$ for all $(u, v) \in E$, then all stable equilibria are edge-cohesive. If y_v^* satisfies $\frac{y_v^* \pi}{M} \leq \gamma$ for all $v \in V$, then all stable equilibria are node-cohesive.

Sections IV-C and IV-E give sufficient conditions for existence of stable cohesive equilibria and non-existence of stable non-cohesive equilibria; together, these constitute sufficient conditions for global practical synchronization from a given set of inputs. In the following section, we present an approach for selecting inputs that satisfy these conditions.

V. SUBMODULAR OPTIMIZATION APPROACH TO INPUT SELECTION

In this section, we present our submodular optimization approach to selecting a set of input nodes to guarantee practical node or edge synchronization from almost any initial state. Our approach is based on ensuring that the conditions for existence of a cohesive equilibrium (Section IV-C) and non-existence of stable non-cohesive equilibria (Section IV-E) are satisfied.

Section V-A formulates the condition for existence of a cohesive equilibrium as a submodular constraint on the input set. We first define an augmented graph and prove that the conditions for existence shown in Section IV-C are equivalent to connectivity of a class of random subgraphs of the augmented graph. We then show that this connectivity condition can be expressed as a constraint of the form $h(A) = n$, where h is a submodular function. We recall that a function $h : 2^V \rightarrow \mathbb{R}$ is *submodular* if, for any sets A and B with $A \subseteq B$ and any $v \notin B$,

$$h(A \cup \{v\}) - h(A) \geq h(B \cup \{v\}) - h(B).$$

Section V-B formulates non-existence of stable non-cohesive equilibria as a submodular constraint on the input set. As in Section V-A, we first construct an augmented graph, although the construction of this section differs from Section V-B. We then prove that the conditions identified in Section IV-E are equivalent to connectivity of a class of subgraphs of the augmented graph, and show that this connectivity condition is equivalent to a submodular constraint on the input set.

In Section V-C, we formulate the problem of selecting a set of input nodes to achieve practical synchronization as an optimization problem that combines the constraints of Sections V-A and V-B. We then present algorithms for selecting a set of input nodes and analyze the optimality guarantees of those algorithms.

A. Submodular Constraint for Cohesive Equilibrium Existence

We first define an augmented network graph, and then describe the sufficient condition for existence of a cohesive

equilibrium based on the augmented graph. We then prove that selecting a set of input nodes to satisfy this condition can be formulated as a submodular constraint.

Let $M \in \mathbb{Z}^+$ as in Section IV-C. The augmented graph $G' = (V', E')$ consists of a set of nodes

$$V' = \{v_m : m = 0, \dots, M, v \in V\} \\ \cup \{(u, v)_r : r = 0, \dots, M, (u, v) \in E\}.$$

The augmented graph is directed, with $(x, y) \in E'$ if there is a directed edge from node x to node y . The set $N(v_m)$ denotes the set of nodes with outgoing edges to v_m . The neighbor set of node v_m is defined by

$$N(v_m) = \{u_l : u \in N(v), l = 0, \dots, M\} \cup \{v_l : l < m\} \\ \cup \{(u, v)_r : u \in N(v), r = 0, \dots, M\}.$$

The set $N((u, v)_r)$ denotes the set of nodes with outgoing edges to $((u, v)_r)$, and is defined by

$$N((u, v)_r) = \{u_l : l = 0, \dots, r\} \cup \{v_m : m = 0, \dots, r\} \\ \cup \{(u, v)_{r'} : r' < r\} \\ \cup \{(\hat{u}, v)_s : \hat{u} \in N(v), s = 0, \dots, M\} \\ \cup \{(\hat{u}, \hat{v})_s : \hat{v} \in N(u), s = 0, \dots, M\}$$

We define a subset of V' , denoted V'_0 , by $V'_0 = \{v_0 : v \in A\} \cup \{v_M : v \notin A\}$. We now define a class of subgraphs of G' that will be used to formulate our sufficient conditions for existence of cohesive equilibria.

Definition 7: A subgraph $\tilde{G} \subseteq G'$ is of *class \mathcal{T}* if the neighbor sets satisfy the following properties. For each node v_m , the neighbor set is a set $\mathcal{T}(v_m)$ satisfying

$$\sum_{u \in N(v)} K_{uv} \left[\sum_{u_l \in \mathcal{T}(v_m)} \alpha_1(m, l) \right] \\ > \sum_{u \in N(v)} K_{uv} \left[\sum_{u_l \in N(v_m)} \alpha_1(m, l) \right] \\ - (|\omega_v| - \bar{K}_v \beta_1(m, M)), \quad (19)$$

where $\bar{K}_v = \sum_{u \in N(v)} K_{uv}$, $\beta_1(m, l)$ is defined as in Section IV-C, and $\alpha_1(m, l) = \beta_1(m, l) - \beta_1(m, l+1)$. Furthermore, for each $u \in N(v)$, if $u_l \notin \mathcal{T}(v_m)$, then $(u, v)_{m-l-1} \in \mathcal{T}(v_m)$. Finally, $v_{m'} \in \mathcal{T}(v_m)$ for all $m' < m$.

For each node $(u, v)_r$, the neighbor set $\mathcal{T}((u, v)_r)$ satisfies

$$\sum_{(\hat{u}, v)_s \in \mathcal{T}((u, v)_r)} K_{\hat{u}v} \alpha_3(s) > \sum_{(\hat{u}, v)_s \in N((u, v)_r)} K_{\hat{u}v} \alpha_3(s) \\ - (\tau_v - (\bar{K}_v - K_{uv}) \beta_3(M) - K_{uv} \beta_2(r)) \quad (20)$$

$$\sum_{(\hat{u}, v)_s \in \mathcal{T}((u, v)_r)} K_{\hat{u}v} \alpha_3(s) > \sum_{(\hat{u}, v)_s \in N((u, v)_r)} K_{\hat{u}v} \alpha_3(s) \\ - (\tau_u - (\bar{K}_u - K_{uv}) \beta_3(M) - K_{uv} \beta_2(r)) \quad (21)$$

where $\alpha_3(s) = \beta_3(s) - \beta_3(s+1)$. Finally, for each $l = 0, \dots, r$, exactly one of u_l or v_{r-l-1} is in $\mathcal{T}((u, v)_r)$, and $\{(u, v)_{r'} : r' < r\} \subseteq \mathcal{T}((u, v)_r)$.

We now define a sufficient condition for existence of cohesive equilibria based on the class \mathcal{T} subgraphs.

Theorem 6: In the algorithm of Section IV-C, $v \in S$ if and only if, for each class \mathcal{T} subgraph \tilde{G} , there exists a directed path from at least one node in V'_0 to v_{M-1} . We have $(u, v) \in S$ if and only if, for each class \mathcal{T} subgraph \tilde{G} , there exists a directed path from at least one node in V'_0 to $(u, v)_{M-1}$.

Proof: We first prove that if $v \in S$, then there exists a directed path from at least one node in V'_0 to v_{M-1} , and that if $(u, v) \in S$, then there exists a directed path from at least one node in V'_0 to $(u, v)_{M-1}$, in each class \mathcal{T} subgraph of V' . Our approach is to prove by induction on k that, at each iteration k , the nodes

$$T[k] = \{v_m : m \geq x_v[k]\} \cup \{(u, v)_r : r \geq x_{uv}[k]\}$$

are connected to V'_0 in each class \mathcal{T} subgraph. At iteration $k = 0$, $T[0] = V'_0$.

Suppose that, at iteration k , node v satisfies $x_v[k] = x_v[k-1] - 1$. Suppose first that

$$\sum_{u \in N(v)} K_{uv} \beta_1(x_v[k-1], x_u[k-1]) > |\omega_v| \quad (22)$$

holds. Setting $m = x_v[k-1]$, Eq. (22) can be rewritten as

$$\sum_{u \in N(v)} \sum_{l=x_u[k-1]}^{M-1} K_{uv} \alpha_1(m, l) > -\bar{K}_v \beta_1(m, M) + |\omega_v|,$$

which is equivalent to

$$\sum_{u_l \in N(v_m) \cap T[k]} K_{uv} \alpha_1(m, l) \geq -\bar{K}_v \beta_1(m, M) + |\omega_v|.$$

Now, if \tilde{G} is a class \mathcal{T} subgraph, then we have that $\mathcal{T}(v_m)$ satisfies (19). Combining these equations yields

$$\sum_{u_l \in N(v_m) \cap T[k]} K_{uv} \alpha_1(m, l) + \sum_{u_l \in \mathcal{T}(v_m)} K_{uv} \alpha_1(m, l) \\ > \sum_{u_l \in N(v_m)} K_{uv} \alpha_1(m, l).$$

Since $K_{uv} \alpha_1(m, l) \geq 0$ for all u, v, m , and l , we must have $T[k] \cap \mathcal{T}(v_m) \neq \emptyset$. By inductive hypothesis, each node in $T[k]$ is connected to a node in V'_0 , and hence v_m is connected to V'_0 .

Now suppose that $x_u[k-1] + x_{uv}[k-1] < x_v[k-1]$. Let $l = x_u[k-1]$ and $r = x_{uv}[k-1]$. By induction, both u_l and $(u, v)_r$ are connected to V'_0 . By definition of class \mathcal{T} subgraph, either $u_l \in \mathcal{T}(v_m)$ or $(u, v)_{m-l-1} \in \mathcal{T}(v_m)$ and $(u, v)_r$ is connected to $(u, v)_{m-l-1}$. Hence v_m is connected to V'_0 in this case.

If at iteration k , an edge (u, v) satisfies $x_{uv}[k] = x_{uv}[k-1] - 1$, then we have

$$\beta_2(x_{uv}[k-1]) + \sum_{\hat{u} \in N(v) \setminus \{u\}} \beta_3(x_{\hat{u}v}[k-1]) \geq \frac{|\omega_v|}{K} \quad (23)$$

if (6) holds (the case where (7) holds is similar). The expression can be rewritten as

$$\begin{aligned} & \sum_{(\hat{u}, v)_s \in N(v_m) \cap T[k]} K_{\hat{u}v} \alpha_3(s) \\ & + \sum_{(\hat{u}, v)_s \in \mathcal{T}((u, v)_r)} K_{\hat{u}v} \alpha_3(s) \\ & > \sum_{(\hat{u}, v)_s \in N((u, v)_r)} K_{\hat{u}v} \alpha_3(s), \end{aligned}$$

which implies that $T[k] \cap \mathcal{T}((u, v)_r) \neq \emptyset$. By induction $T[k]$ is connected to V'_0 , and hence $(u, v)_r$ is connected to V'_0 as well.

Finally, if $x_u[k-1] + x_v[k-1] < x_{uv}[k-1]$, let $l = x_u[k-1]$ and $m = x_v[k-1]$. We have that either $u_l \in \mathcal{T}((u, v)_r)$ or $v_{r-l-1} \in \mathcal{T}((u, v)_r)$ and v_m is connected to v_{r-l-1} . Since u_l and v_m are both connected to V'_0 by induction, $(u, v)_r$ is connected to V'_0 . This completes the proof that if $v \in S$ (resp. $(u, v) \in S$), then V'_0 is connected to v_{M-1} (resp. $(u, v)_{M-1}$) in any class \mathcal{T} subgraph of V' .

We now show that if v_{M-1} is connected to V'_0 in every class \mathcal{T} subgraph of V' , then $v \in S$. We first assume that $v \notin S$, and then construct a class \mathcal{T} subgraph in which V'_0 is not connected to v_{M-1} . In particular, we construct the set of nodes that are connected to v_{M-1} , denoted \mathcal{D} , and prove that $\mathcal{D} \cap V'_0 = \emptyset$.

Initialize the set $\mathcal{D} \subseteq V'$ as $\mathcal{D} = \{v_{M-1}\}$. Since $v \notin S$, we have that

$$\sum_{u \in N(v)} K_{uv} \beta_1(M, x_u^*) < |\omega_v|,$$

and hence

$$\sum_{u \in N(v)} \sum_{l=x_u^*}^{M-1} K_{uv} \alpha_1(M, l) < |\omega_v| - \bar{K}_v \beta_1(M, M).$$

Letting $\mathcal{T}(v_{M-1}) = \{u_l \in N(v_{M-1}) : l < x_u^*\}$, we have that $\mathcal{T}(v_{M-1})$ satisfies (19). Finally, for all $u_l \notin \mathcal{T}(v_m)$ with $u \in N(v)$, add $(u, v)_{m-l-1}$ to $\mathcal{T}(v_m)$; since $x_v^* > m$, $x_{uv}^* > m - l - 1$.

Setting $\mathcal{D} = \mathcal{D} \cup \mathcal{T}(v_{M-1})$, we have that \mathcal{D} consists of nodes u_l that satisfy $x_u^* > l$ and $u_l \notin V'_0$. Proceeding via induction, we select a node $u_l \in \mathcal{D}$ such that the neighbor set $\mathcal{T}(u_l)$ has not been assigned yet. We have that u_l satisfies

$$\sum_{s \in N(u)} \sum_{l'=x_s^*}^{M-1} K_{su} \alpha_1(l, l') < |\omega_v| - \bar{K}_u \beta_1(l, M).$$

By a similar argument to the above, we select $\mathcal{T}(u_l) = \{s_{l'} \in N(u_l) : l' < x_s^*\}$. We then set $\mathcal{D} = \mathcal{D} \cup \mathcal{T}(u_l)$, noting that the properties $x_s^* > l'$ for $s_{l'} \in \mathcal{D}$ and $\mathcal{D} \cap V'_0 = \emptyset$ have been preserved.

If all nodes $u_l \in \mathcal{D}$ have had $\mathcal{T}(u_l)$ assigned, select a node $(u, v)_r \in \mathcal{D}$ such that $\mathcal{T}((u, v)_r)$ has not been assigned. By induction, $r < x_{uv}^*$, and hence

$$\sum_{\hat{u} \in N(v) \setminus \{u\}} K_{\hat{u}v} \beta_3(x_{\hat{u}v}^*) > |\omega_v| - K_{uv} \beta_2(r)$$

and

$$\sum_{\hat{v} \in N(u) \setminus \{v\}} K_{u\hat{v}} \beta_3(x_{u\hat{v}}^*) > |\omega_u| - K_{uv} \beta_2(r).$$

We therefore set $\mathcal{T}((u, v)_r) = \{(\hat{u}, v)_s : s < x_{\hat{u}v}^*\} \cup \{(u, \hat{v})_s : s < x_{u\hat{v}}^*\}$, and note that $\mathcal{T}((u, v)_r)$ satisfies the criteria for a class \mathcal{T} subgraph. Finally, since $r < x_{uv}^*$, for each l either $x_u^* > l$ (in which case, add u_l to $\mathcal{T}(v_m)$) or $x_v^* > r - l$ (in which case, add v_{r-l} to $\mathcal{T}(v_m)$). If all nodes in \mathcal{D} have had their neighbor sets assigned, then the procedure terminates.

At the end of this procedure, we have a class \mathcal{T} subgraph \tilde{G} and a set of nodes \mathcal{D} , which consists of all nodes that are connected to v_{M-1} in \tilde{G} . Since $\mathcal{D} \cap V'_0 = \emptyset$ by induction, V'_0 is not connected to v_{M-1} . This proves the other direction of the theorem. ■

The following corollary gives explicit conditions for existence of node and edge cohesive equilibria based on the connectivity of class \mathcal{T} subgraphs.

Corollary 3: Suppose that a class \mathcal{T} subgraph of G' is chosen at random, according to a probability distribution that assigns nonzero weight to each class \mathcal{T} subgraph. If each node $\{v_{M-1} : v \in V\}$ is connected to V'_0 with probability one, then a node cohesive equilibrium exists. If each node $\{(u, v)_{M-1} : (u, v) \in E\}$ is connected to V'_0 with probability one, then an edge cohesive equilibrium exists.

The following known result will lead to a submodular constraint for existence of cohesive equilibria.

Lemma 7 ([33]): Let $G = (V, E)$ be a directed graph, and let $A \subseteq V$ and $U \subseteq V$. Define $f(A)$ to be the expected number of nodes in U that are connected to A in a random subgraph of G with known distribution. Then $f(A)$ is submodular as a function of A .

Combining Lemma 7 with Corollary 3 yields the following.

Lemma 8: Let A denote the set of input nodes, and let $r_1(A)$ denote the expected number of nodes in $\{v_{M-1} : v \in V\}$ that are connected to V'_0 in a randomly chosen class \mathcal{T} subgraph. Then $r_1(A)$ is submodular as a function of A . If $r_1(A) = n$, then a node cohesive equilibrium exists.

Proof: The submodularity of $r_1(A)$ follows from Lemma 7. If $r_1(A) = n$, then for any class \mathcal{T} subgraph of G' , all nodes in $\{v_{M-1} : v \in V\}$ are connected to at least one node in A . The existence of an edge cohesive equilibrium follows from Theorem 6. ■

Analogously, if we define $r'_1(A)$ to be the expected number of nodes in $\{(u, v)_{M-1} : (u, v) \in E\}$ that are connected to V'_0 in a randomly chosen class \mathcal{T} subgraph, then $r'_1(A) = p$, where $p = |E|$ as in Section III-A, implies the existence of an edge cohesive equilibrium, and $r'_1(A)$ is submodular.

B. Submodular Constraint for Non-Existence of Non-Cohesive Equilibria

In this section, we present a submodular constraint on the set of input nodes for guaranteeing non-existence of non-node cohesive and non-edge cohesive equilibria. As in Section V-A, our approach is to construct an augmented graph and prove that the desired property is equivalent to connectivity of a random subgraph of the augmented graph.

Let $\beta_i^\lambda(m, l)$ be defined as in Section IV-E. We define $\alpha_i^\lambda(m, l) = \beta_1^\lambda(m, l) - \beta_1^\lambda(m, l + 1)$ and $\alpha_i^\lambda(r) = \beta_i^\lambda(r) - \beta_i^\lambda(r + 1)$ for $i = 2, 3$. Let $M \in \mathbb{Z}^+$. The vertex set of the augmented graph is given by

$$V'' = \{v_m : m = 0, \dots, M\} \cup \{(u, v)_r : (u, v) \in E, r = 0, \dots, M\}.$$

The nodes v_m represent whether node v has all stable equilibria in the region $|\theta_v| \leq \frac{\pi m}{M}$, while the nodes $\{(u, v)_r\}$ represent whether all stable equilibria satisfy $|f(\theta_v - \theta_u)| \leq \frac{\pi r}{M}$.

The edge set E'' of the graph is defined by assigning the following neighbor sets to each node. For each node v_m , the neighbor set is given by

$$N(v_m) = \{v_{m'} : m' < m\} \cup \{u_l : u \in N(v), l = 0, \dots, M\} \cup \{(u, v)_r : u \in N(v), r = 0, \dots, m\}.$$

The nodes $(u, v)_r$ have neighbor sets defined by

$$\begin{aligned} N((u, v)_r) = & \{(u, v)_{r'} : r' < r\} \\ & \cup \{(\hat{u}, v)_s : \hat{u} \in N(v) \setminus \{u\}, s = 0, \dots, M\} \\ & \cup \{(u, \hat{v})_s : \hat{v} \in N(u) \setminus \{v\}, s = 0, \dots, M\} \\ & \cup \{u_l : l = 0, \dots, r\} \cup \{v_m : m = 0, \dots, r\} \end{aligned}$$

Define

$$V_0'' = \{v_0 : v \in A\} \cup \{v_M : v \notin A\} \cup \{(u, v)_M : (u, v) \in E\}.$$

We now define a *class \mathcal{U} subgraph* of the augmented graph $G'' = (V'', E'')$. We will show that sufficient conditions for non-existence of non-cohesive stable equilibria can be formulated based on the connectivity of randomly-chosen class \mathcal{U} subgraphs of G'' .

Definition 8: A subgraph $\tilde{G} = (\tilde{V}, \tilde{E})$ is a class \mathcal{U} subgraph of G'' if $\tilde{V} = V''$ and the neighbor sets satisfy the following properties. Let $\Psi = \{\lambda_1, \dots, \lambda_R\} \subset [0, \infty]$. For each node $v_m \in V''$ and $\lambda \in \Psi$, the neighbor set $\mathcal{U}(v_m)$ satisfies

$$\begin{aligned} & \sum_{u_l \in \mathcal{U}(v_m)} K_{uv} \alpha_1^\lambda(m, l) \\ & \geq \sum_{u_l \in N(v_m)} K_{uv} \alpha_1^\lambda(m, l) + \bar{K}_v \beta_1^\lambda(m, M) - \tau_{\lambda, v}. \end{aligned} \quad (24)$$

For each $u \in N(v)$ and $l = 0, \dots, m$, if $u_l \notin \mathcal{U}(v_m)$, then $(u, v)_{m-l-1} \in \mathcal{U}(v_m)$. Finally, $\{v_{m'} : m' < m\} \subseteq \mathcal{U}(v_m)$.

For each node $(u, v)_r \in V''$, the neighbor set $\mathcal{U}((u, v)_r)$ satisfies

$$\begin{aligned} & \sum_{\hat{u} \in N(v) \setminus \{u\}} \sum_{(u, v)_s \in \mathcal{U}((u, v)_r)} K_{\hat{u}v} \alpha_2^\lambda(s) \\ & \geq K_{uv} \beta_3^\lambda(0) + (\bar{K}_v - K_{uv})(\beta_2^\lambda(0) - \beta_2^\lambda(M)) \\ & \quad - \tau_{\lambda, v} - K_{uv} \beta_3^\lambda(r) \end{aligned} \quad (25)$$

$$\begin{aligned} & \sum_{\hat{v} \in N(u) \setminus \{v\}} \sum_{(u, \hat{v})_s \in \mathcal{U}((u, v)_r)} K_{u\hat{v}} \alpha_2^\lambda(s) \\ & \geq K_{uv} \beta_3^\lambda(0) + (\bar{K}_v - K_{uv})(\beta_2^\lambda(0) - \beta_2^\lambda(M)) \\ & \quad - K_{uv} \beta_2^\lambda(M) - \tau_{\lambda, u} - \beta_3^\lambda(r) \end{aligned} \quad (26)$$

For each $l = 0, \dots, r$, either $u_l \in \mathcal{U}((u, v)_r)$ or $v_{r-l-1} \in \mathcal{U}((u, v)_r)$. Finally, $\{(u, v)_{r'} : r' < r\} \subseteq \mathcal{U}((u, v)_r)$.

In the definition of the neighbor set $\mathcal{U}(v_m)$, each constraint (24) is related to one of the constraints (13) of Section IV-E. Similarly, the constraints (25) and (26) map to the constraints (14) and (15) of Section IV-E. Formally, this connection is established by the following theorem, which relates the non-existence of stable non-cohesive equilibria to the connectivity of class \mathcal{U} subgraphs.

Theorem 7: Consider the algorithm of Section IV-E. The final index value of node v , y_v^* , satisfies $y_v^* \leq m$ if and only if v_m is connected to V_0'' in all class \mathcal{U} subgraphs.

Proof: We first show that if $y_v^* \leq m$, then v_m is connected to V_0'' in all class \mathcal{U} subgraphs. Our approach is to prove that, at each iteration k of the algorithm, $m = y_v[k]$ implies that v_m is connected to V_0'' and $r = y_{uv}[k]$ implies that $(u, v)_r$ is connected to V_0'' . At iteration 0, the result follows from the definition of V_0'' and the initialization of the algorithm.

At iteration k , let

$$T[k] = \{v_m : m \geq y_v[k]\} \cup \{(u, v)_r : r \geq y_{uv}[k]\}.$$

Suppose that v satisfies $y_v[k] = y_v[k-1] - 1$ and let $m = y_v[k]$. If (13) holds, then we have

$$\sum_{u \in N(v)} K_{uv} \beta_1^\lambda(y_v[k-1], y_u[k-1]) > \tau_{\lambda, v}.$$

Applying a telescoping sum argument yields

$$\sum_{u \in N(v)} K_{uv} \left[\sum_{l=y_u[k-1]}^{M-1} \alpha_1^\lambda(m, l) + \beta_1^\lambda(m, M) \right] > \tau_{\lambda, v}.$$

By rearranging terms and using the definition of $T[k]$, we have

$$\sum_{u_l \in T[k] \cap N(v_m)} K_{uv} \alpha_1^\lambda(m, l) > \tau_{\lambda, v} - \bar{K}_v \beta_1^\lambda(m, M). \quad (27)$$

Adding (24) and (27) yields

$$\begin{aligned} & \sum_{u_l \in T[k] \cap N(v_m)} K_{uv} \alpha_1^\lambda(m, l) + \sum_{u_l \in \mathcal{U}(v_m)} K_{uv} \alpha_1^\lambda(m, l) \\ & > \sum_{u_l \in N(v_m)} K_{uv} \alpha_1^\lambda(m, l). \end{aligned}$$

Since $K_{uv} \alpha_1^\lambda(m, l) \geq 0$ and $(T[k] \cap N(v_m))$ and $\mathcal{U}(v_m)$ are both subsets of $N(v_m)$, we must have $T[k] \cap \mathcal{U}(v_m) \neq \emptyset$. Since $T[k]$ is connected to V_0'' by inductive hypothesis, v_m is connected to V_0'' in \tilde{G} .

If $y_{uv}[k-1] + y_u[k-1] < m$ for some $u \in N(v)$, then let $r = y_{uv}[k-1]$ and $l = y_u[k-1]$. By induction, both $(u, v)_r$ and u_l are connected to V_0'' . Furthermore, by definition of $\mathcal{U}(v_m)$, either $(u, v)_r$ or u_{m-r-1} is in $\mathcal{U}(v_m)$. If $(u, v)_r \in \mathcal{U}(v_m)$, v_m is connected to V_0'' . If $u_{m-r-1} \in \mathcal{U}(v_m)$, then $l \leq m - r - 1$ implies that V_0'' is connected to u_l and u_l is connected to v_m . Hence v_m is connected to V_0'' .

Now, suppose that an edge $(u, v) \in E$ satisfies $y_{uv}[k] = y_{uv}[k-1] - 1$. Let $r = y_{uv}[k]$. We show that $(u, v)_r$ is connected to V_0'' . If (14) holds for some $\lambda \in \Psi$, then

$$K_{uv} \beta_2^\lambda(r) + \sum_{\hat{u} \in N(v) \setminus \{u\}} K_{\hat{u}v} \beta_3^\lambda(y_{\hat{u}v}[k-1]) > \tau_{\lambda, v}.$$

A telescoping sum argument implies that

$$K_{uv}\beta_2^\lambda(r) + \sum_{\hat{u} \in N(v) \setminus \{u\}} K_{\hat{u}v} \left[\sum_{s=y_{\hat{u}v}[k-1]}^{M-1} \alpha_3^\lambda(s) \right] > \tau_{\lambda,v}. \quad (28)$$

Adding (25) and (28) and rearranging terms gives

$$\begin{aligned} & \sum_{\hat{u} \in N(v) \setminus \{u\}} \sum_{(\hat{u},v)_s \in T[k]} K_{\hat{u}v} \alpha_3^\lambda(s) \\ & + \sum_{\hat{u} \in N(v) \setminus \{u\}} \sum_{(\hat{u},v)_s \in \mathcal{U}((u,v)_r)} K_{\hat{u}v} \alpha_3^\lambda(s) \\ & > \sum_{\hat{u} \in N(v) \setminus \{u\}} \sum_{(\hat{u},v)_s \in N(v_m)} K_{\hat{u}v} \alpha_3^\lambda(s). \end{aligned} \quad (29)$$

Hence $T[k] \cap \mathcal{U}((u,v)_r) \neq \emptyset$, and so $(u,v)_r$ is connected to V_0'' . A similar argument establishes connectivity if (15) holds.

If $y_u[k-1] + y_v[k-1] < r$, let $y_u[k-1] = l$ and $y_v[k-1] = m$. Either $u_l \in \mathcal{U}((u,v)_r)$, in which case $(u,v)_r$ is connected to V_0'' , or $v_{r-l-1} \in \mathcal{U}((u,v)_r)$. In the latter case, $y_v[k-1] \leq (r-l-1)$ implies that V_0'' is connected to v_m , which is in turn connected to $(u,v)_r$.

To show the other direction of the theorem, suppose that $y_v^* > m$. We will construct a class \mathcal{U} subgraph \tilde{G} such that v_m is not connected to V_0'' . Let \mathcal{D} be a subset of V'' and initialize $\mathcal{D} = \{v_m\}$. The set \mathcal{D} will be equal to the set of nodes that are connected to v_m in \tilde{G} ; we will grow \mathcal{D} through an iterative procedure and prove that, upon termination of the procedure, $\mathcal{D} \cap V_0'' = \emptyset$, and hence v_m is not connected to V_0'' .

First, we define $\mathcal{U}(v_m) = \{u_l : l < x_u^*\}$. We will show that $\mathcal{U}(v_m)$ satisfies (24). Since $m < x_v^*$, we have

$$\sum_{u \in N(v)} K_{uv} \beta_1^\lambda(m, x_u^*) < |\omega_v|.$$

Writing $\beta_1^\lambda(m, x_u^*)$ as a telescoping sum gives

$$\sum_{u \in N(v)} K_{uv} \left[\sum_{l=x_u^*}^{M-1} \alpha_1^\lambda(m, l) + \beta_1^\lambda(m, M) \right] < |\omega_v|.$$

Adding

$$\sum_{u \in N(v)} \sum_{l=0}^{x_u^*-1} K_{uv} \alpha_1^\lambda(m, l)$$

to both sides and rearranging terms gives

$$\begin{aligned} & \sum_{u \in N(v)} \sum_{l=0}^{x_u^*-1} K_{uv} \alpha_1^\lambda(m, l) \\ & > \sum_{u \in N(v)} \sum_{l=0}^{M-1} K_{uv} \alpha_1^\lambda(m, l) - (|\omega_v| - \bar{K}_v \beta_1^\lambda(m, M)), \end{aligned}$$

implying that (24) holds with $\mathcal{U}(v_m) = \{u_l : l < x_u^*\}$.

In order to fully define $\mathcal{U}(v_m)$, for each $l = 0, \dots, m$, if $l > y_u^*$, we add $(u, v)_{m-l-1}$ to $\mathcal{U}(v_m)$. Since $y_v^* > m$,

$$m < y_v^* < (y_{uv}^* + y_u^*) < y_{uv}^* + l,$$

and hence $y_{uv}^* > m - l > m - l - 1$. Set $\mathcal{D} = \mathcal{D} \cup \mathcal{U}(v_m)$.

We proceed by induction. At each step, we have a set \mathcal{D} consisting of elements that are connected to v_m in \tilde{G} , do not belong to V_0'' , and are of the form u_l for some $l < y_u^*$ or $(u, v)_r$ for $r < y_{uv}^*$. Select an element $u_l \in \mathcal{D}$ and choose its neighbor set as $\mathcal{U}(u_l) = \{w_s : w \in N(u), s < y_w^*\}$. By the argument given above, $\mathcal{U}(u_l)$ satisfies (24). Set $\mathcal{D} = \mathcal{D} \cup \mathcal{U}(u_l)$.

If neighbor sets have been assigned to all nodes $u_l \in \mathcal{D}$, select a node $(u, w)_r \in \mathcal{D}$. The neighbor set $\mathcal{U}((u, w)_r)$ is defined by

$$\begin{aligned} \mathcal{U}((u, w)_r) = & \bigcup_{\hat{w} \in N(u) \setminus \{w\}} \{(u, \hat{w})_s : s < y_{u\hat{w}}^*\} \\ & \cup \left(\bigcup_{\hat{u} \in N(w) \setminus \{u\}} \{(\hat{u}, w)_s : s < y_{\hat{u}w}^*\} \right) \end{aligned}$$

By induction, $r < y_{uw}^*$. Hence (14) does not hold, and

$$\sum_{\hat{w} \in N(u) \setminus \{w\}} K_{u\hat{w}} \beta_2^\lambda(y_{u\hat{w}}^*) < \tau_{u,\lambda} - K_{uw} \beta_3^\lambda(r).$$

Employing a telescoping sum gives

$$\begin{aligned} & \sum_{\hat{w} \in N(u) \setminus \{w\}} K_{u\hat{w}} \left[\sum_{s=y_{u\hat{w}}^*}^{M-1} \alpha_2^\lambda(s) + \alpha_2^\lambda(M) \right] \\ & < \tau_{\lambda,u} - K_{uw} \beta_3^\lambda(r). \end{aligned}$$

Adding

$$\sum_{\hat{w} \in N(u) \setminus \{w\}} \sum_{l=0}^{y_{u\hat{w}}^*-1} K_{u\hat{w}} \alpha_2^\lambda(s)$$

to both sides and rearranging terms yields

$$\begin{aligned} & \sum_{\hat{w} \in N(u) \setminus \{w\}} \sum_{l=0}^{y_{u\hat{w}}^*-1} K_{u\hat{w}} \alpha_2^\lambda(s) \\ & > \sum_{\hat{w} \in N(u) \setminus \{w\}} \sum_{s=0}^{M-1} K_{u\hat{w}} \alpha_2^\lambda(s) - (\tau_{\lambda,u} - K_{uw} \beta_3^\lambda(r)), \end{aligned}$$

and so $\mathcal{U}((u, w)_r)$ satisfies (25). The proof that (26) holds is similar. We then set $\mathcal{D} = \mathcal{D} \cup \mathcal{U}((u, w)_r)$ and continue.

At the end of the inductive procedure, we have a set \mathcal{D} consisting of all nodes that are connected to v_m . By induction, $\mathcal{D} \cap V_0'' = \emptyset$, and so we have constructed a class \mathcal{U} subgraph in which V_0'' is not connected to v_m . ■

Theorem 7 gives conditions on the stable equilibria of (2) based on the connectivity of class \mathcal{U} subgraphs of G'' . The following corollary gives conditions for non-existence of non-cohesive equilibria based on Theorem 7.

Corollary 4: Let $m = \lfloor \frac{M\gamma}{\pi} \rfloor$. Then all stable equilibria are node-cohesive if v_m is connected to V_0'' in all class \mathcal{U} subgraphs. All stable equilibria are edge-cohesive if $(u, v)_m$ is connected to V_0'' in all class \mathcal{U} subgraphs.

The following corollary restates these conditions in terms of random class \mathcal{U} subgraphs.

Corollary 5: Let $m = \lfloor \frac{M\gamma}{\pi} \rfloor$. Suppose that a class \mathcal{U} subgraph is chosen at random from a probability distribution that assigns nonzero weight to each class \mathcal{U} subgraph. Then all

stable equilibria are node-cohesive if v_m is connected to V_0'' for all $v \in V$ with probability 1, and all stable equilibria are edge-cohesive if $(u, v)_m$ is connected to V_0'' for all $(u, v) \in E$ with probability 1.

Define $r_2(A)$ to be the expected number of nodes in $\{v_m : m = \lfloor \frac{M\gamma}{\pi} \rfloor\}$ that are connected to V_0'' when the input set is A , and define $r'_2(A)$ to be the expected number of nodes in $\{(u, v)_m : m = \lfloor \frac{M\gamma}{\pi} \rfloor\}$ that are connected to V_0'' when the input set is A . By Lemma 7, $r_2(A)$ and $r'_2(A)$ are submodular as functions of A . The following lemma gives sufficient conditions for non-existence of non-cohesive stable equilibria based on $r_2(A)$ and $r'_2(A)$.

Lemma 9: All equilibria are node-cohesive if $r_2(A) = n$. All equilibria are edge-cohesive if $r'_2(A) = p$.

Proof: By Corollary 5, all stable equilibria are node-cohesive if all nodes in $\{v_m : m = \lfloor \frac{M\gamma}{\pi} \rfloor\}$ are connected to V_0'' with probability 1 in any random class \mathcal{U} subgraph. Equivalently, all stable equilibria are node-cohesive if the expected number of nodes that are connected to V_0'' in any randomly chosen class \mathcal{U} subgraph is N , i.e., $r_1(A) = n$. The proof that all equilibria are edge-cohesive if $r'_2(A) = p$ is similar. ■

Having derived constraints for existence of cohesive equilibria and non-existence of non-cohesive equilibria, we next combine these constraints to formulate selecting a set of input nodes to achieve practical synchronization as an optimization problem. We present algorithms that exploit the submodular structure of these constraints to provide provable optimality bounds.

C. Selecting Inputs for Practical Synchronization

By combining the conditions derived in Sections V-A and V-B, we have that the nodes achieve practical node synchronization if $r_1(A) + r_2(A) = 2n$ and practical edge synchronization if $r'_1(A) + r'_2(A) = 2p$.

We consider two problems based on these constraints. In the first problem, we select the minimum-size set of input nodes in order to guarantee practical node (resp. edge) synchronization. In the second problem, we select a set of up to k input nodes in order to maximize the level of synchronization.

In the case of ensuring practical node synchronization, the first problem can be formulated as

$$\begin{aligned} & \text{minimize} && |A| \\ & \text{s.t.} && r_1(A) + r_2(A) = 2n \end{aligned} \quad (30)$$

The problem of guaranteeing practical edge synchronization has an analogous formulation with $r'_1(A)$ and $r'_2(A)$ replacing $r_1(A)$ and $r_2(A)$, respectively.

The solution to (30) can be approximated by initializing the set $A = \emptyset$ and, at each iteration, adding the node v to A that maximizes $r_1(A \cup \{v\}) + r_2(A \cup \{v\})$. The algorithm terminates when $r_1(A) + r_2(A) = 2n$. The following lemma gives an optimality bound for this approach.

Lemma 10: Let A_{k-1} denote the set of input nodes at the second-to-last iteration of the algorithm, let A denote the set that is returned, and let A^* denote the minimum-size set of

inputs to satisfy the conditions of Lemmas 8 and 9. Then

$$\frac{|A_k|}{|A^*|} \leq 1 + \ln \left(\frac{n}{r_1(A) + r_2(A) - r_1(A_{k-1}) - r_2(A_{k-1})} \right).$$

Proof: The lemma follows from the submodularity of r_1 and r_2 , and Theorem 1 of [34]. ■

The problem of selecting up to k input nodes in order to maximize node synchronization can be formulated as

$$\begin{aligned} & \text{maximize} && r_1(A) + r_2(A) \\ & \text{s.t.} && |A| \leq k \end{aligned} \quad (31)$$

In order to approximate (31), a greedy procedure analogous to the algorithm for (30) is as follows. Initialize the set $A = \emptyset$. At each iteration, add the node v to A that maximizes $r_1(A \cup \{v\}) + r_2(A \cup \{v\})$. The algorithm terminates after k iterations, when $|A| = k$. The optimality bounds of this algorithm is described by the following lemma.

Lemma 11: Let A^* denote the optimal solution to (31), and let \hat{A} denote the set of inputs chosen by the greedy algorithm. Then $r_1(\hat{A}) + r_2(\hat{A}) \geq (1 - \frac{1}{e})(r_1(A^*) + r_2(A^*))$.

Proof: The proof follows from submodularity of $r_1(A) + r_2(A)$ and [35, Theorem 4.1]. ■

We observe that, since the number of class \mathcal{T} and \mathcal{U} subgraphs is large in general, the objective functions $r_1(A)$, $r_2(A)$, $r'_1(A)$, and $r'_2(A)$ can be approximated by generating a set of random class \mathcal{T} and \mathcal{U} subgraphs according to some probability distribution.

VI. NUMERICAL RESULTS

We investigated our approach through a numerical study. The goal of our study was to analyze the impact of the external inputs on the oscillator dynamics, as well as to investigate the properties of the inputs chosen by our algorithm. We considered synchronization in three application domains: (i) synchronization of phase angles in the IEEE 14 Bus power system test case [15], (ii) time synchronization in wireless networks [28], modeled as a geometric random graph, and (iii) synchronization of firing rates in the *C. Elegans* neuronal network [16]. The results of each study are summarized as follows. In all cases, the constant $M = 10$ and the number of random subgraphs used to compute $r_1(A)$ and $r_2(A)$ was equal to 20.

A. Phase Synchronization in Power System

Synchronization plays a vital role in the power system, in which stable operation requires buses and generators to maintain the same frequency and a relative phase difference of no more than $\pi/2$ on each transmission line (edge) [36]. In order to evaluate our approach to synchronization of power systems, we consider the first-order model (2) with negligible resistance on the transmission lines. The input nodes represent generators that are fixed to a common reference phase and frequency in order to restore stability to the grid. We studied phase synchronization in the power system using the IEEE 14 Bus case study [15], which provides a network topology with $n = 14$ nodes along with the line impedances of the edges. We defined the coupling coefficient $K_{uv} = 1/\eta_{uv}$, where

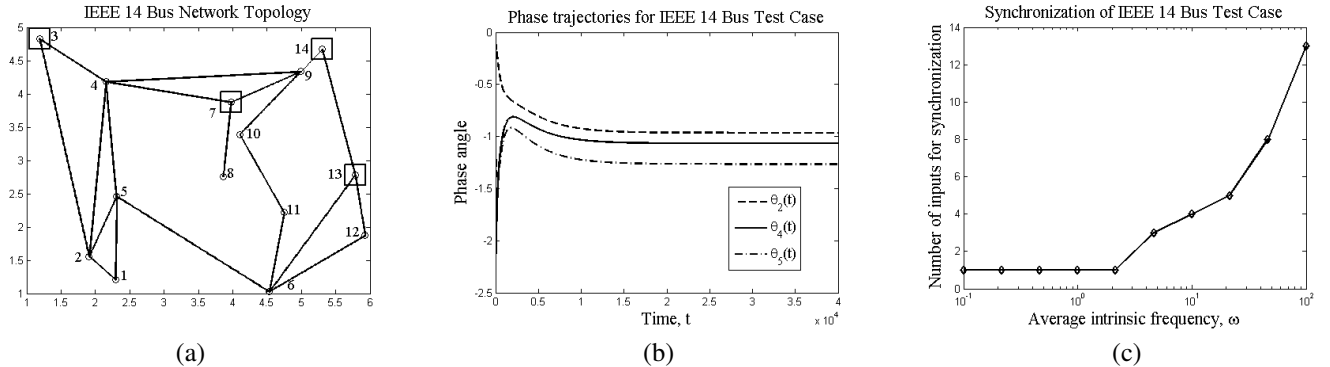


Fig. 1. Synchronization case study using the IEEE 14 Bus case study [15]. Coupling coefficients were chosen to be equal to the inverse of the magnitudes of the line impedances, while the intrinsic frequencies were chosen from a Gaussian distribution. (a) Illustration of 14-bus network and inputs needed for one trial when the variance of the intrinsic frequencies was equal to 10. The black squares indicate input nodes. (b) Sample trajectories for nodes 2, 4, and 5 in the 14-bus network. Node trajectories converge to within the desired phase difference ($\gamma = \pi/2$) of each other. (c) Number of inputs required for practical edge synchronization as a function of the variance of the intrinsic frequencies. As the variance increases, the frequencies of neighboring nodes diverge and hence more inputs are needed to ensure synchronization.

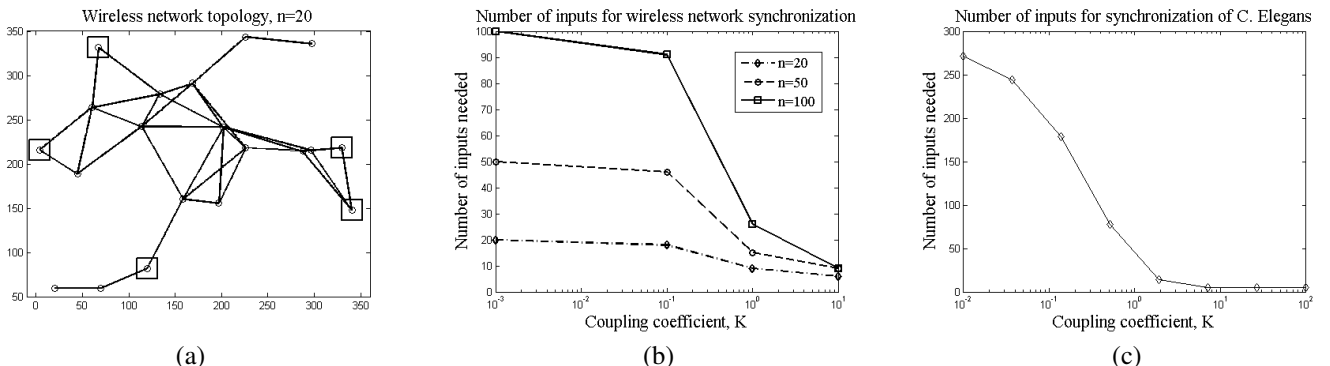


Fig. 2. Numerical results for time synchronization and neuronal synchronization. (a) Illustration of inputs chosen for a wireless network, modeled as a geometric random graph, when $K = 0.7197$, $n = 20$, and the input nodes are indicated by squares. The set of input nodes is based on the network topology and intrinsic frequencies of the nodes. (b) Number of input nodes required for time synchronization. The number of nodes is a decreasing function of the coupling coefficient. The reduction in the fraction of input nodes required for synchronization is most significant for larger network size. (c) Number of input nodes required for synchronization of the *C. Elegans* network ($n = 279$) when the intrinsic frequencies have Gaussian distribution with unit variance. The number of inputs is a decreasing function of the coupling coefficient.

η_{uv} is the magnitude of the impedance of edge (u, v) . The intrinsic frequencies were chosen according to a zero-mean Gaussian distribution with variance ranging from 0.01 to 100 in different trials. The goal was to ensure that the phase angles satisfied $|\theta_v - \theta_u| < \frac{\pi}{2}$ (i.e., edge-cohesiveness with $\gamma = \pi/2$), consistent with the goal of guaranteeing power system stability [36].

Figure 1(a) illustrates input selection for a given set of intrinsic frequencies. The variance of the intrinsic frequencies was equal to 10. The dark squares indicate input nodes selected by our algorithm ($|A| = 4$). We observe that each non-input node is at most two hops away from an input node, which suggests that centrally located nodes are more likely to be candidates for inputs. On the other hand, nodes with high degree were not necessarily chosen as inputs. Additional information beyond the network topology, including the intrinsic frequencies and the coupling coefficients between nodes, is incorporated into the input selection process.

In Figure 1(b), trajectories of nodes 2, 4, and 5 from Figure 1(a) are shown. The trajectories of these neighboring nodes converge to within the desired bound of $\frac{\pi}{2}$ from each other, and synchronize to the frequency of the input nodes ($\omega_0 = 0$;

by Lemma 1, an arbitrary initial frequency could be chosen, but we selected $\omega_0 = 0$ for clarity of the figure). Practical edge synchronization occurs in spite of the fact that the initial phases of neighboring nodes 2 and 5 differed by more than $\pi/2$.

Figure 1(c) shows the number of input nodes required to achieve practical synchronization for different intrinsic frequencies. When the variance of $\{\omega_v : v \in V\}$ is low, only one input node is required to achieve synchronization. For variance near 10, an intermediate number of inputs is required for synchronization, while for large variance in the intrinsic frequencies all nodes must be selected as input nodes to guarantee synchronization.

B. Time Synchronization

We analyzed time synchronization in wireless networks, in which the input nodes represent anchor nodes with clocks that are set to the reference time. We modeled the wireless network as a geometric random graph. Each node was assumed to share an edge with other nodes within a range of 100m. The simulation was run with the number of nodes $n = \{20, 50, 100\}$. The nodes were assumed to be deployed uniformly at random

over a square region, with area chosen so that each node had three neighbors on average. Nodes were assumed to have i.i.d. Gaussian intrinsic frequency with unit variance and zero mean. We computed the number of input nodes required to ensure practical node synchronization with $\gamma = \pi/4$ of each other. The edges had identical coupling with $K_{uv} = K$ for all $(u, v) \in E$, with K in the set $\{0.01, 0.01, 0.1, 1, 10\}$.

Figure 2(a) shows one example of a geometric random graph with $n = 20$ and $K = 0.7197$ for all links. The input nodes are indicated by black squares. As in the power system case study, most non-input nodes are within two hops of an input node, and high-degree nodes are not necessarily chosen as inputs. Two adjacent nodes are both chosen as inputs, due to the high intrinsic frequencies of those nodes.

The number of nodes required for synchronization is shown in Figure 2(b). The number of nodes required for synchronization is a decreasing function of the coupling coefficient, since a stronger coupling implies that input nodes are able to steer their neighbors into the cohesive region. We observe that the fraction of input nodes required for synchronization is smaller for larger networks.

C. Firing Rate Synchronization in Neuronal Network

Synchronization of groups of neuronal cells to a common frequency plays a role in information storage and processing for motor control [37] and memory [3]. We analyzed the impact of input nodes on synchronization using the *Caenorhabditis Elegans* (roundworm) neuronal network [16]. The number of nodes is $n = 279$. The intrinsic frequencies were independently from a zero-mean, unit-variance Gaussian distribution. All links had the same coupling coefficient K , which varied from $K = 0.001$ to $K = 10$. The goal was to achieve practical node synchronization with $\gamma = \pi/4$.

We observed that the number of input nodes required decreases as the coupling coefficient increases. The reduction in the number of nodes required was larger than in the random geometric graph (Section VI-B), even though the neuronal network contained more nodes. An explanation for this phenomenon is that the neuronal network has higher degree, as well as additional links between different regions of the network. This more connected network topology enables synchronization of more nodes and at a lower coupling coefficient.

VII. CONCLUSIONS AND FUTURE WORK

We considered the problem of ensuring practical synchronization of phase-coupled oscillators from any initial state by introducing external input nodes. We studied two synchronization problems. In the first problem, the goal is for all node phases to converge to within a bound of a given reference phase, while also converging to the same frequency. In the second problem, the relative phase differences between neighboring nodes must converge to a given bound, while all nodes converge to the same frequency.

We derived sufficient conditions for achieving both synchronization goals. We proved that each synchronization criterion is achieved if there exists at least one equilibrium that lies

within the desired region (either all nodes within a given bound of the reference phase, or all relative differences within a given bound), and no stable equilibria outside the desired region. We then presented a threshold-based condition for existence of an equilibrium within the desired region, as well as an efficient algorithm for verifying existence of such an equilibrium. Finally, we derived a class of conditions for non-existence of stable equilibria outside the desired region, and proposed an algorithm for verifying non-existence of undesired equilibria for a given set of input nodes.

We formulated a submodular optimization approach for selecting a set of input nodes to guarantee synchronization. To achieve a submodular formulation, we first constructed an augmented network graph. We identified two classes of subgraphs (denoted class \mathcal{T} and class \mathcal{U}) of the augmented graph. We proved that the sufficient condition for existence of a desired equilibrium is equivalent to connectivity between each non-input node and the input set in all class \mathcal{T} subgraphs. We then showed that the sufficient conditions for non-existence of undesired equilibria are equivalent to connectivity between each non-input node and the input set in all class \mathcal{U} subgraphs.

We mapped this condition to submodular constraints on the set of input nodes. Based on the submodular formulation, we proposed efficient algorithms with provable optimality bounds for selecting a set of up to k nodes in order to maximize the level of synchronization in the network, as well as selecting the minimum-size input set to guarantee a desired level of synchronization.

Our approach was validated through a numerical study of synchronization in power system, wireless, and neuronal networks. Our numerical study supports the intuition that the number of input nodes required decreases as the coupling between neighboring nodes grows stronger. In addition, we found that centrally located nodes are often chosen as inputs, so that the maximum distance between a node and the input set is small.

The threshold-based conditions derived in this work are sufficient, but not necessary. Characterizing the space of networks where these conditions are also necessary, as well as developing tighter sufficient conditions, remains an open problem. Furthermore, while the model we studied considers the first-order dynamics of the nodes, second-order dynamics are often used to model systems such as the power grid [20]. Generalizing our approach to these second-order systems is a direction of future research.

REFERENCES

- [1] F. Dörfler and F. Bullo, "Synchronization and transient stability in power networks and nonuniform Kuramoto oscillators," *SIAM Journal on Control and Optimization*, vol. 50, no. 3, pp. 1616–1642, 2012.
- [2] R. Eckhorn, R. Bauer, W. Jordan, M. Brosch, W. Kruse, M. Munk, and H. Reitboeck, "Coherent oscillations: A mechanism of feature linking in the visual cortex?" *Biological Cybernetics*, vol. 60, no. 2, pp. 121–130, 1988.
- [3] W. Klimesch, "Memory processes, brain oscillations and EEG synchronization," *International Journal of Psychophysiology*, vol. 24, no. 1, pp. 61–100, 1996.
- [4] D. A. Paley, N. E. Leonard, R. Sepulchre, D. Grunbaum, and J. K. Parrish, "Oscillator models and collective motion," *IEEE Control Systems*, vol. 27, no. 4, pp. 89–105, 2007.

[5] A. Arenas, A. Díaz-Guilera, J. Kurths, Y. Moreno, and C. Zhou, "Synchronization in complex networks," *Physics Reports*, vol. 469, no. 3, pp. 93–153, 2008.

[6] M. G. Rosenblum, A. S. Pikovsky, and J. Kurths, "Phase synchronization of chaotic oscillators," *Physical Review Letters*, vol. 76, no. 11, p. 1804, 1996.

[7] J. A. Acebrón, L. L. Bonilla, C. J. P. Vicente, F. Ritort, and R. Spigler, "The Kuramoto model: A simple paradigm for synchronization phenomena," *Reviews of Modern Physics*, vol. 77, no. 1, p. 137, 2005.

[8] S. H. Strogatz, "From Kuramoto to Crawford: exploring the onset of synchronization in populations of coupled oscillators," *Physica D: Nonlinear Phenomena*, vol. 143, no. 1, pp. 1–20, 2000.

[9] A. Jadbabaie, N. Motee, and M. Barahona, "On the stability of the Kuramoto model of coupled nonlinear oscillators," *Proceedings of the American Control Conference (ACC)*, vol. 5, pp. 4296–4301, 2004.

[10] N. Chopra and M. W. Spong, "On exponential synchronization of Kuramoto oscillators," *IEEE Transactions on Automatic Control*, vol. 54, no. 2, pp. 353–357, 2009.

[11] L. M. Childs and S. H. Strogatz, "Stability diagram for the forced Kuramoto model," *Chaos: An Interdisciplinary Journal of Nonlinear Science*, vol. 18, 2008.

[12] C. C. McIntyre and P. J. Hahn, "Network perspectives on the mechanisms of deep brain stimulation," *Neurobiology of Disease*, vol. 38, no. 3, pp. 329–337, 2010.

[13] Y. Wang and F. J. Doyle, "Exponential synchronization rate of Kuramoto oscillators in the presence of a pacemaker," *IEEE Transactions on Automatic Control*, vol. 58, no. 4, pp. 989–994, 2013.

[14] H. Kori and A. S. Mikhailov, "Entrainment of randomly coupled oscillator networks by a pacemaker," *Physical Review Letters*, vol. 93, no. 25, p. 254101, 2004.

[15] "Data sheets for IEEE 14 bus system," http://shodhganga.inflibnet.ac.in/bitstream/10603/5247/18/19_appendix.pdf.

[16] L. R. Varshney, B. L. Chen, E. Paniagua, D. H. Hall, and D. B. Chklovskii, "Structural properties of the *Caenorhabditis Elegans* neuronal network," *PLoS Computational Biology*, vol. 7, no. 2, 2011.

[17] A. T. Winfree, "Biological rhythms and the behavior of populations of coupled oscillators," *Journal of Theoretical Biology*, vol. 16, no. 1, pp. 15–42, 1967.

[18] Y. Kuramoto, "Self-entrainment of a population of coupled non-linear oscillators," *International Symposium on Mathematical Problems in Theoretical Physics*, pp. 420–422, 1975.

[19] P. Monzón and F. Paganini, "Global considerations on the Kuramoto model of sinusoidally coupled oscillators," *Proceedings of the 44th IEEE Conference on Decision and Control and European Control Conference (CDC-ECC)*, pp. 3923–3928, 2005.

[20] F. Dörfler, M. Chertkov, and F. Bullo, "Synchronization in complex oscillator networks and smart grids," *Proceedings of the National Academy of Sciences*, vol. 110, no. 6, pp. 2005–2010, 2013.

[21] D. A. Wiley, S. H. Strogatz, and M. Girvan, "The size of the sync basin," *Chaos: An Interdisciplinary Journal of Nonlinear Science*, vol. 16, 2006.

[22] O. V. Popovych and P. A. Tass, "Macroscopic entrainment of periodically forced oscillatory ensembles," *Progress in Biophysics and Molecular Biology*, vol. 105, no. 1, pp. 98–108, 2011.

[23] A. Clark, B. Alomair, L. Bushnell, and R. Poovendran, "A submodular optimization approach to global synchronization of Kuramoto oscillators," *Submitted to American Control Conference (ACC)*, 2015.

[24] Y. Liu, J. Slotine, and A. Barabási, "Controllability of complex networks," *Nature*, vol. 473, no. 7346, pp. 167–173, 2011.

[25] J. Rouths and D. Rouths, "Control profiles of complex networks," *Science*, vol. 343, pp. 1373–1376, 2014.

[26] N. E. Leonard, T. Shen, B. Nabet, L. Scardovi, I. D. Couzin, and S. A. Levin, "Decision versus compromise for animal groups in motion," *Proceedings of the National Academy of Sciences*, vol. 109, no. 1, pp. 227–232, 2012.

[27] D. C. Michaels, E. P. Matyas, and J. Jalife, "Mechanisms of sinoatrial pacemaker synchronization: a new hypothesis," *Circulation Research*, vol. 61, no. 5, pp. 704–714, 1987.

[28] R. Baldoni, A. Corsaro, L. Querzoni, S. Scipioni, and S. T. Piergiovanni, "Coupling-based internal clock synchronization for large-scale dynamic distributed systems," *IEEE Transactions on Parallel and Distributed Systems*, vol. 21, no. 5, pp. 607–619, 2010.

[29] G. Filatrella, A. H. Nielsen, and N. F. Pedersen, "Analysis of a power grid using a Kuramoto-like model," *The European Physical Journal B-Condensed Matter and Complex Systems*, vol. 61, no. 4, pp. 485–491, 2008.

[30] L. Moreau, "Stability of continuous-time distributed consensus algorithms," *Proceedings of the 43rd IEEE Conference on Decision and Control (CDC)*, vol. 4, pp. 3998–4003, 2004.

[31] H. K. Khalil and J. Grizzle, *Nonlinear Systems*. Prentice Hall Upper Saddle River, 2002.

[32] W. Basener, B. P. Brooks, and D. Ross, "The Brouwer fixed point theorem applied to rumour transmission," *Applied Mathematics Letters*, vol. 19, no. 8, pp. 841–842, 2006.

[33] D. Kempe, J. Kleinberg, and É. Tardos, "Maximizing the spread of influence through a social network," *Proceedings of the 9th ACM SIGKDD International Conference on Knowledge Discovery and Data Mining*, pp. 137–146, 2003.

[34] L. Wolsey, "An analysis of the greedy algorithm for the submodular set covering problem," *Combinatorica*, vol. 2, no. 4, pp. 385–393, 1982.

[35] G. Nemhauser, L. Wolsey, and M. Fisher, "An analysis of approximations for maximizing submodular set functions - I," *Mathematical Programming*, vol. 14, no. 1, pp. 265–294, 1978.

[36] A. R. Bergen, *Power Systems Analysis*. Pearson Education India, 2009.

[37] M. Cassidy, P. Mazzone, A. Oliviero, A. Insola, P. Tonali, V. Di Lazzaro, and P. Brown, "Movement-related changes in synchronization in the human basal ganglia," *Brain*, vol. 125, no. 6, pp. 1235–1246, 2002.